Handout

IC 62 Treatment strategy for the custom ablation of visually disturbing irregular astigmatism after refractive surgery and in keratoconus

Senior Instructor: A. Stojanovic

Co Instructors: R. Ambrósio Jr
D. Reinstein
M. Mrochen
A. Kanellopoulos
X. Chen

The text and surgery material & video for this course is available at:

http://www.laservision.gr/en/escrscourse_handouts2013

Website: www.laservision.gr

https://www.facebook.com/LaserVision.gr

https://www.youtube.com/user/Laservision07

https://twitter.com/laservisiongr

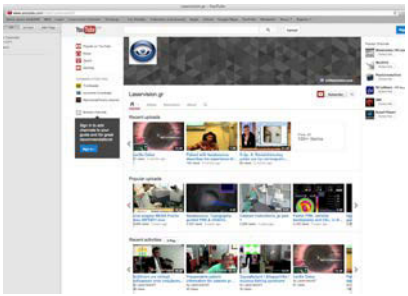

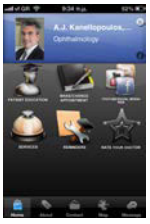

Search for **Kanellopoulos App** (iphone & android)
Apple: https://itunes.apple.com/us/app/kanellopoulos-eye-center/id620285571?ls=1&mt=8

Android:https://play.google.com/store/apps/details?id=com.cloudninedevelopmentllc.AJohnKanellopoloulos_151

Course Description: How to plan your "last shot" with custom ablation for your unhappy patient who underwent various types of treatments/retreatments? Choosing the right treatment strategy is essential in eyes with weakened corneas and small amount of tissue available for custom ablation after complicated refractive surgery or in keratoconus. The leading experts will present latest advances in corneal diagnostics including corneal structural and biomechanical analysis, as well as the ablation planning on various platforms with or without corneal collagen cross-linking. A decision tree with practical guidelines of "dos and don'ts" will be presented. The surgeons with first hand experience with various commercially available systems will conduct an interactive discussion of their successful and failed cases. Limitations and pitfalls will be identified.

Course Objectives: To gain familiarity with necessary diagnostic methods and treatment options for custom ablation of visually disturbing irregular astigmatism. Special attention will be taken on measures for staying on the safe side when treating these high-risk cases.

Course Schedule: 1. Michael Mrochen: o Technological requirements and practical guidelines for relevant diagnostics, ablation planning and treatment of irregular astigmatism (15 minutes) o A decision tree in custom ablation treatment of complex cases (10 minutes) 2. Dan Reinstein: o Corneal structural analysis of complicated corneas using Artemis VHF digital ultrasound scanning (15 minutes) o Treatment of complex cases combining internal corneal anatomical data with an excimer laser (10 minutes) 3. Renato Ambrosio Jr: o Assessing the corneal biomechanical properties and anterior segment metrics to determine the amount and placement of possible custom ablation for regularizing the irregular corneal optics (10 minutes) o Clinical experience in the treatment of complex cases with the WaveLight system (10 minutes) 4. Aleksandar Stojanovic: o Strategic planning in custom ablation of irregular astigmatism. Where can we compromise when we need to ration with corneal tissue? (10 minutes) o Clinical experience in the treatment of complex cases with the iVis system (10 minutes) 5. A. John Kanellopoulos: o Athens protocol (topography-guided partial PRK and CXL) in the management of keratoconus and post LASIK ectasia (20 minutes) 6. Xiangjun Chen: o Transepithelial topo-guided ablation in the treatment of LASIK flap or interface complication with visually disturbing irregular astigmatism and/or scattering (10 minutes)

Clinical Ophthalmology

Dovepress
open access to scientific and medical research

Open Access Full Text Article

CASE SERIES

Topography-guided hyperopic and hyperopic astigmatism femtosecond laser-assisted LASIK: long-term experience with the 400 Hz eye-Q excimer platform

This article was published in the following Dove Press journal:
Clinical Ophthalmology
11 June 2012
Number of times this article has been viewed

Anastasios John Kanellopoulos

Department of Ophthalmology, New York University Medical School, New York, NY, and LaserVision.gr Eye Institute, Athens, Greece

Background: The purpose of this study was to evaluate the safety and efficacy of topography-guided ablation using the WaveLight 400 Hz excimer laser in laser-assisted in situ keratomileusis (LASIK) for hyperopia and/or hyperopic astigmatism.

Methods: We prospectively evaluated 208 consecutive LASIK cases for hyperopia with or without astigmatism using the topography-guided platform of the 400 Hz Eye-Q excimer system. The mean preoperative sphere value was +3.04 ± 1.75 (range 0.75–7.25) diopters (D) and the mean cylinder value was −1.24 ± 1.41 (−4.75–0) D. Flaps were created either with Intralase FS60 (AMO, Irvine, CA) or FS200 (Alcon, Fort Worth, TX) femtosecond lasers. Parameters evaluated included age, preoperative and postoperative refractive error, uncorrected distance visual acuity, corrected distance visual acuity, flap diameter and thickness, topographic changes, higher order aberration changes, and low contrast sensitivity. These measurements were repeated postoperatively at regular intervals for at least 24 months.

Results: Two hundred and two eyes were available for follow-up at 24 months. Uncorrected distance visual acuity improved from 5.5/10 to 9.2/10. At 24 (8–37) months, 75.5% of the eyes were in the ±0.50 D range and 94.4% were in the ±1.00 D range of the refractive goal. Postoperatively, the mean sphere value was −0.39 ± 0.3 and the cylinder value was −0.35 ± 0.25. Topographic evidence showed that ablation was made in the visual axis and not in the center of the cornea, thus correlating with the angle kappa. No significant complications were encountered in this small group of patients.

Conclusion: Hyperopic LASIK utilizing the topography-guided platform of the 400 Hz Eye-Q Allegretto excimer and a femtosecond laser flap appears to be safe and effective for correction of hyperopia and/or hyperopic astigmatism. The results are impressive for refractive error correction and stability and for improvement of both uncorrected and corrected distance visual acuity.

Keywords: topography-guided, LASIK, hyperopia, hyperopic astigmatism, mixed astigmatism, angle kappa

Video abstract

Point your SmartPhone at the code above. If you have a QR code reader the video abstract will appear. Or use: http://dvpr.es/Mlzvr6

Correspondence: Anastasios John Kanellopoulos
LaserVision.gr Eye Institute, Tsocha 17
Ampelokipi, Athens 11527, Greece
Tel +30 21 0747 2777
Fax +30 21 0747 2789
Email ajk@brilliantvision.com

Introduction

The evolution of laser technology has enabled treatment of myopic, hyperopic, and astigmatic eyes to become more accurate. There have been several reports of hyperopic laser-assisted in situ keratomileusis (LASIK) in the past.[1–11] We have previously reported on the use of standard wavefront-optimized excimer ablations in hyperopic LASIK with good results[12] and on the use of topography-guided excimer ablations.[13,14] Hyperopic patients invariably have a significant angle kappa.[15] We have anecdotally observed clinically superior visual axis centration in hyperopes when

© 2012 Kanellopoulos, publisher and licensee Dove Medical Press Ltd. This is an Open Access article which permits unrestricted noncommercial use, provided the original work is properly cited.

topography-guided ablations were attempted. In this study, we evaluated the safety and efficacy of topography-guided LASIK for hyperopia with or without astigmatism.

Materials and methods

Two hundred and eight consecutive eyes from 156 patients underwent LASIK for hyperopia or hyperopic astigmatism. The inclusion criteria were hyperopia +0.25 D to +8.0 D, astigmatism up to –6.0 D, and spherical equivalent +6.0 D at most. Patients with previous corneal surgery, a history of herpetic eye disease, corneal dystrophy, corneal scarring, keratoconus, severe dry eye, or collagen or vascular disease were excluded.

Preoperative evaluation included uncorrected distance visual acuity, refraction (manifest, cycloplegic), best spectacle corrected visual acuity, slit-lamp examination including fundus evaluation, corneal tomographic imaging with Oculyzer Scheimpflug corneal tomography (Alcon, Fort Worth, TX), Topolyzer Placido-disc based topography (Alcon), ultrasound central corneal pachymetry with the Nidek US-1800 (Echoscan, Achi, Japan) and Wavefront analysis with the Allegretto-Wave Tscherning wavefront analyzer (WaveLight Laser Technologie, Erlangen, Germany) measured at a pupil size of 6.5 mm. Contrast sensitivities were also measured using the CSV-1000 (Vector Vision, Arcanum, OH). Our initial pilot experience with 30 eyes had led us to use a customized nomogram-adjustment algorithm for the ablation treatment plan, as shown in Table 1. This was used to compensate for the regression we had encountered in the earlier cases.

The operative technique was as follows. A disposable patient interface was used for each eye treated with femtosecond laser for flap creation. A drop of proparacaine 1% (Alcaine, Alcon) was instilled into the patient's eye just before the procedure. The eyelids were painted with povidone iodine antiseptic 10% (Betadine, Purdue Pharma LP, Stamford, CT),) and the eye lashes were isolated with sterile plastic drapes (Tegaderm, 3M Health Care, St Paul, MN). The femtosecond laser was used to cut the corneal flaps in all cases. The flaps were cut to expose a stromal bed of at least 9.0 mm in diameter and 135 µm in depth, which was sufficiently large for a hyperopic (large diameter) ablation and its accompanying blend zone. Intraoperative flap diameter was measured with a surgical caliper. Ultrasound pachymetry measurement of the residual stromal bed was done with the same corneal pachymeter that had been used preoperatively. This value was subtracted from the preoperative corneal thickness, and the difference was taken as the corneal flap thickness (subtraction pachymetry). The 400 Hz Eye-Q excimer was used to perform ablations in all cases using the topography-guided platform. Images were taken from the Oculyzer (Scheimpflug-based corneal tomography).

Table 1 Nomogram adjustment used for amount of sphere to be corrected

	Dominant eye	Nondominant eye
Sphere	Add +0.25	Add +0.5 to +0.75
Cylinder	Treat all (topoguided)	Treat all (topoguided)

Patients were examined half an hour postoperatively to check for any flap irregularities or complications.

Postoperatively parameters evaluated were uncorrected and corrected distance visual acuity, cornea tomography and topography, manifest refraction, wavefront changes, and contrast sensitivity. These examinations were repeated during follow-up at day 1, week 1, and months 1, 3, and 6. Evaluations were carried out every 6 months thereafter. All surgeries were performed by a single surgeon (AJK) in an outpatient refractive surgery center in Athens, Greece. Measurements and data gathering were undertaken by the surgeon and his associate staff.

Results

Two hundred and two eyes were available for evaluation at two years; three patients were lost to follow-up and five eyes received enhancement procedures prior to completion of our evaluation. The mean age was 40.4 ± 11.8 (range 19–62) years. Males comprised 54% of the cases and females comprised 46%. The mean preoperative sphere value was +3.04 ± 1.75 (range +0. 75 to +7.25) D, and the mean cylinder value was -1.24 ± 1.41 (range from –4.75 to 0) D. Uncorrected distance visual acuity improved from 5.5/10 to 8.2/10. At 24 (8–37) months, 75.5% of the eyes were in the ±0.50 D range of the refractive goal and 94.4% were in the ±1.00 D range. Mean preoperative sphere values were +3.04 ± 1.75 D and the mean preoperative cylinder value was –1.24 ± 1.41; the respective postoperative values were –0.39 ± 0.3 D and –0.35 ± 0.25. There was an increase in best spectacle-corrected visual acuity from 9.1/10 preoperatively to 9.5/10 postoperatively. Figure 3 shows a comparison of preoperative corrected distance visual acuity in blue and postoperative uncorrected distance visual acuity in red, indicating obvious improvement. Figure 4 shows the preoperative cylinder distribution in red and the postoperative cylinder distribution in blue. Figure 5 is a vectogram of preoperative cylinder distribution in blue dots (distance on the y axis represents amount and on the x axis represents

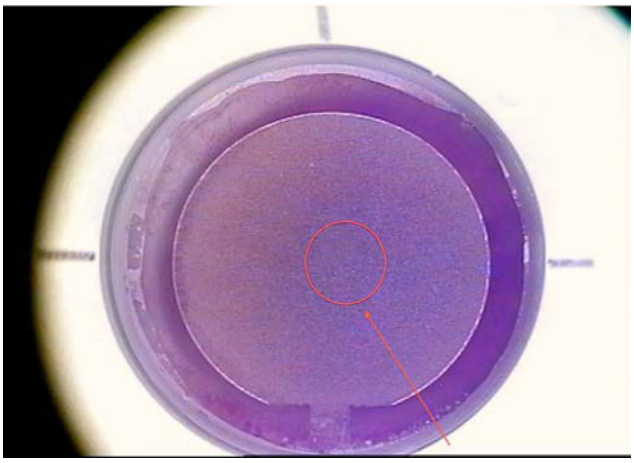

Figure 1 Flap-making report generated by the FS200 femtosecond laser.
Notes: The image of the flap created (right eye, surgeons view) is shown here in reference to the pupil highlighted by the red circle and shown by the red arrow. It is easy to ascertain that this flap has been created nasally in order to accommodate a similarly placed topography-guided ablation.

degrees, with the yellow dots representing the postoperative cylinder vectogram).

Figure 6 shows the predictability graph, with red dots showing overcorrection and blue dots showing undercorrection; the green dots are within ±0.5 D. This graph shows a slight tendency for overcorrection of higher refractive errors, which was our preoperative aim in order to compensate for any long-term regression effect. Figure 7 is the safety graph, with lines gained and lost, indicating a good safety profile with this technique and an impressive 46.6% of cases gaining at least one line of acuity postoperatively. Flap diameter was 8.9 ± 0.2 mm and flap thickness was 135 ± 8 µm, calculated by ultrasonic subtraction pachymetry. The keratometry readings showed an initial decrease within the first month, then demonstrated a progressive slow decline over the first 2 years, suggesting a predictable long-term regression of the initial hyperopic effect (Figure 8).

Figure 9 shows the results of preoperative and postoperative Scheimpflug-generated tomography. The red arrows point to the visual axis and line of sight. It is obvious that when one evaluates centration of the hyperopic ablation achieved in this hyperopic eye, the optical zone appears decentered in reference to the pupillary image (dotted circle). It is nevertheless centered on the visual axis of this eye with a significant angle kappa. The root mean square of higher-order aberrations increased by 15% from a preoperative value of 0.2–0.0 µm to a postoperative value of 0.23 µm at 12 months of follow-up. There was no epithelial downgrowth or any other significant complications noted in this small group. Low contrast sensitivity score results at 12 cycles/degree (column C on the chart) improved from an average preoperative value of 6.4 to 6.8.

Discussion

We have previously shown that a similar Allegretto excimer platform (200 Hz, wavefront-optimized excimer laser platform) can be safe and effective in hyperopic LASIK.[12] We have also shown that hyperopes have a significant angle kappa, and centering their laser correction on the pupil may be a mistake, suggesting that customized approaches to compensate for the angle kappa may be required in hyperopes.[15] In this study, we used a 400 Eye-Q topography-guided platform and a femtosecond laser for flap creation, and found that they can be superior in terms of safety and efficacy when performing hyperopic and hyperopic astigmatic corrections.

Intricacies of topography-guided hyperopic LASIK that we have encountered include the need for wider flap diameters and the difficulty of centering ablation within the stromal area exposed by the femtosecond laser flap. We aimed for slight (1–1.5 mm) nasal decentration, and slight (0.5 mm) superior decentration of the flaps in order to avoid flap edge and/or hinge placement within the ablation

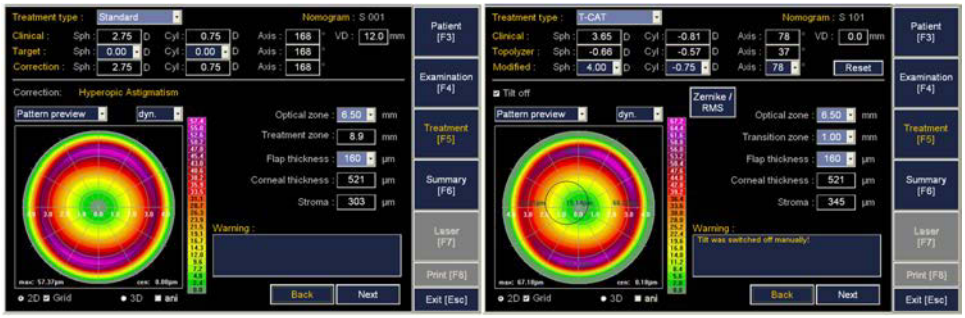

Figure 2 Concept of topography-guided ablation.
Notes: The image on the left shows the relative centration to the pupil image of a standard ablation for +3 diopters in the right eye of a patient. The image on the right shows the exact same correction planned with the topography-guided platform. It is clear that the ablation here appears decentered nasally in reference to the pupillary image (circle).

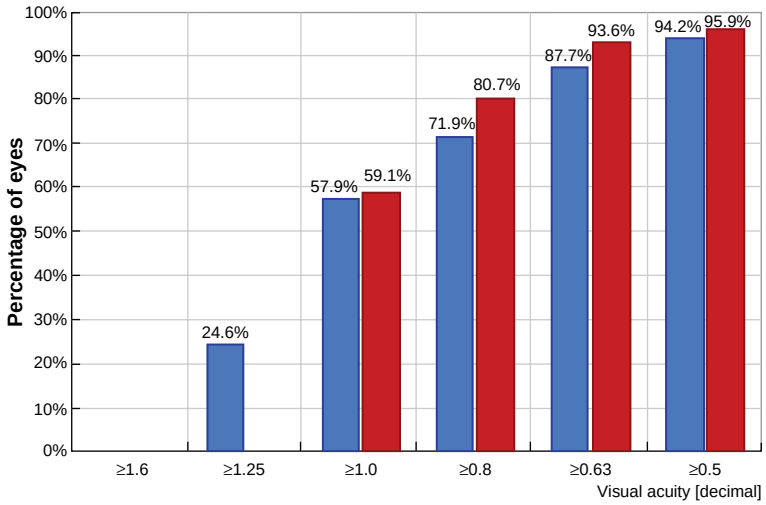

Figure 3 Comparison of preoperative corrected distance visual acuity in blue and postoperative uncorrected distance visual acuity in red, showing obvious improvement.

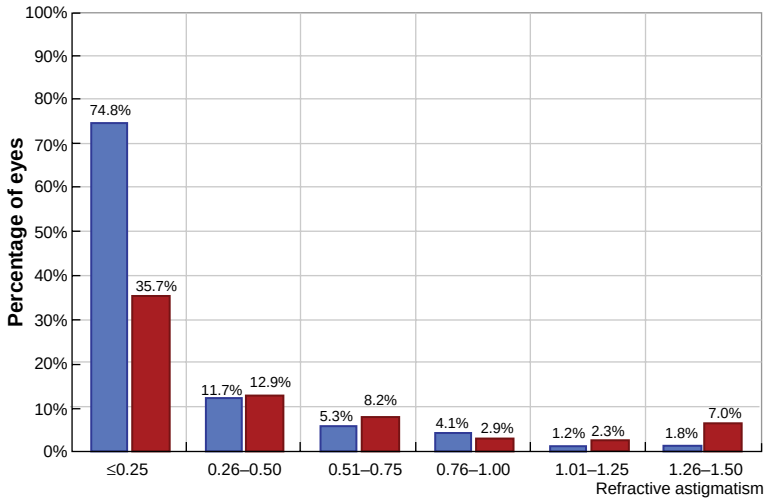

Figure 4 Preoperative (red) and postoperative (blue) cylinder distribution.

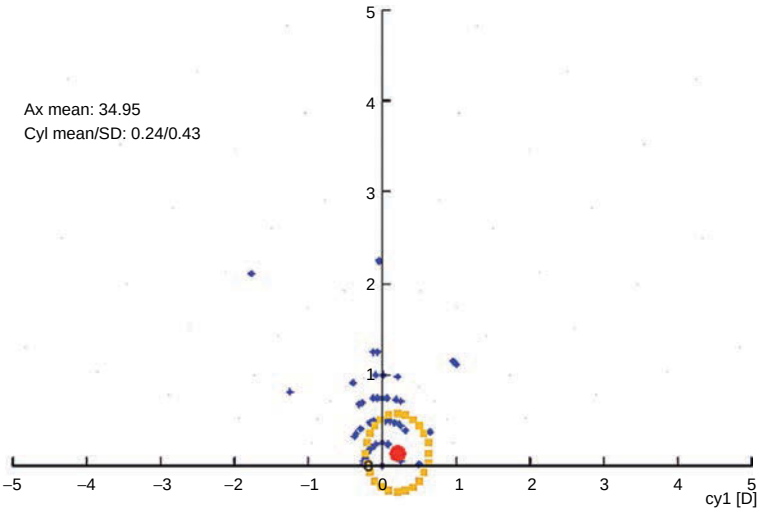

Figure 5 Vectogram of preoperative cylinder distribution in blue dots.
Notes: The distance on the y axis represents amount and the distance on the x axis represents degrees. The yellow dots represent the postoperative cylinder vectogram.

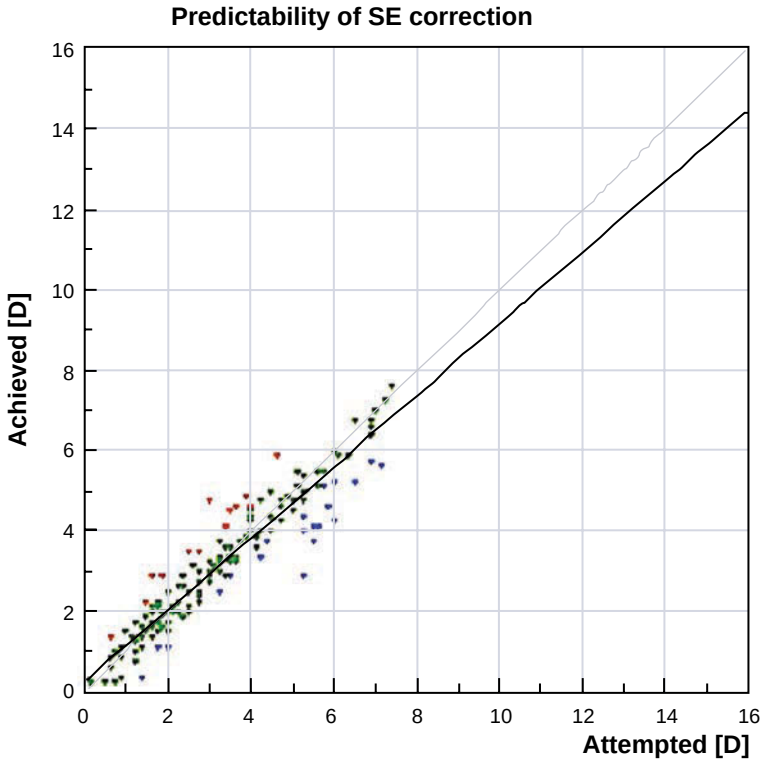

Figure 6 Predictability graph with red dots showing overcorrection and blue dots showing undercorrection, with green dots within ±0.5 diopters.
Notes: This graph shows a slight trend for overcorrection of higher refractive errors, which was our preoperative aim in order to compensate for any long-term regression effect.

zone (Figures 1 and 2). We also calculated the shortest flap diameter to be at least 9 mm in order to achieve adequate ablation (Figure 2).

Some authors have expressed concern about inducing higher order aberrations and astigmatism with hyperopic LASIK ablation.[4,5] No significant wavefront changes occurred in our group. This may be in part attributable to use of the femtosecond laser instead of microkeratome flaps, as has been reported in the past.[16] More than half of our patients gained at least one line of corrected distance visual acuity.

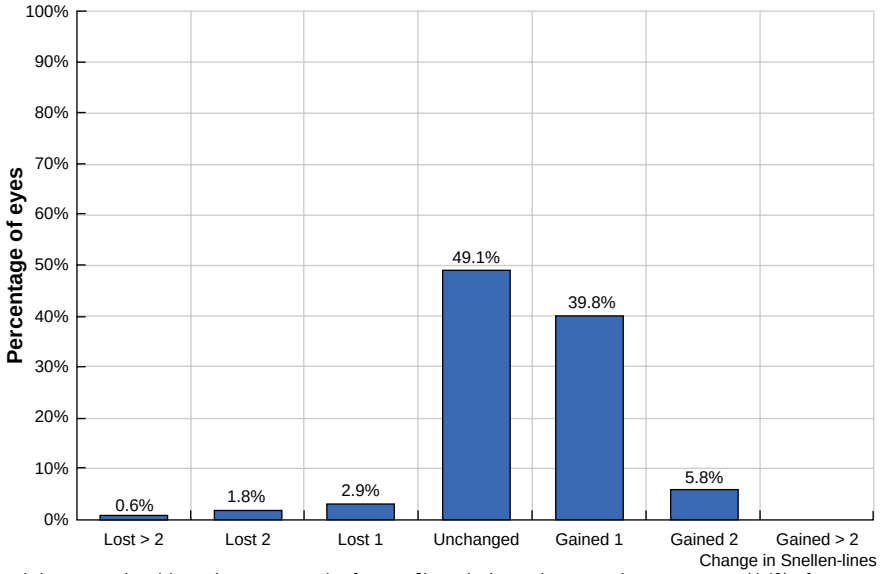

Figure 7 Safety graph with lines gained and lost, showing a good safety profile with this technique and an impressive 46.6% of cases gaining at least one line of acuity postoperatively.

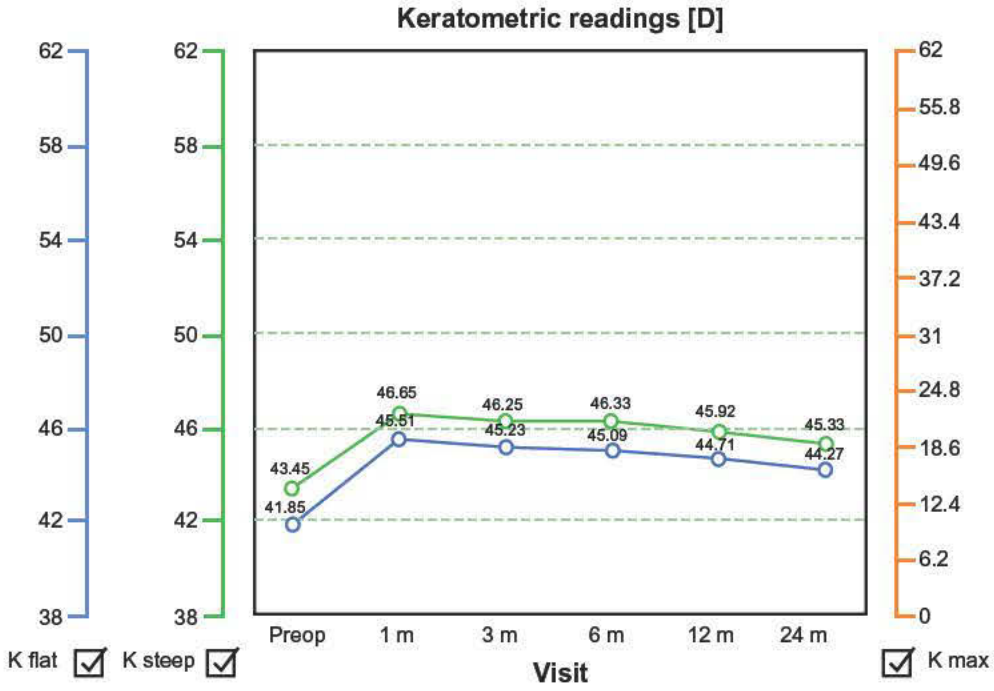

Figure 8 Keratometry readings showed an initial increase within the first month, indicative of effective hyperopic correction, but demonstrated a progressive slow decline over the first 2 years postoperatively, suggesting long-term regression of the initial hyperopic effect.

At 24 months of follow-up, the mean refraction spherical equivalent was ±0.50 D of the intended postoperative refraction in over 80% of cases, which is comparable with or even better than the published results achieved using similar systems for correction of hyperopic refractive errors.[1–11,17] This efficacy also extended to the treatment of mixed hyperopic and astigmatic refractive errors which we theorize may be in part attributable to positive cylinder conversion and treatment of astigmatism on the steep meridian as well as addressing the angle kappa. We consider it inadvisable to perform hyperopic ablations in the center of the pupil, because this will invariably decenter the actual ablation in regard to the visual axis and line of sight, potentially inducing astigmatism. This principle leaves the central optical zone in these procedures untreated by the excimer because both the hyperopia and the cylinder are treated in a theoretical peripheral ring of 6.5–9.5 mm from the center of the visual axis. However, the keratometric regression noted over the average two-year follow-up period suggests that there is an intrinsic biomechanical mechanism in hyperopic LASIK,

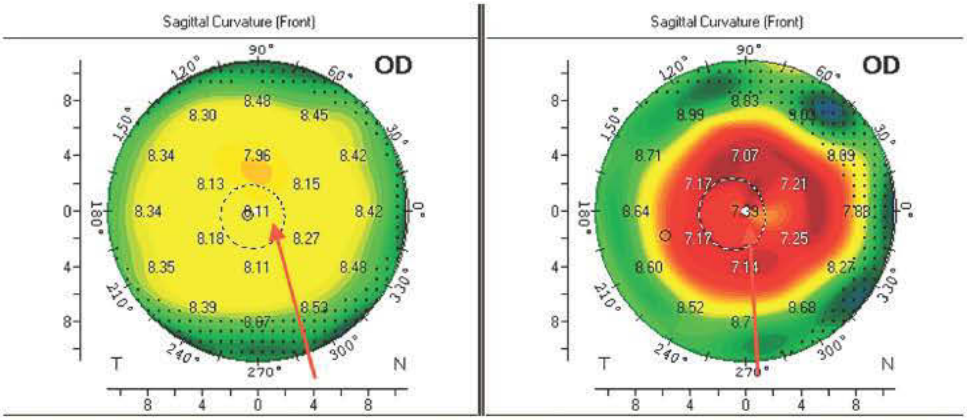

Figure 9 Preoperative and postoperative Scheimpflug-generated tomography.
Notes: The red arrows point to the visual axis and line of sight. It is obvious that when one evaluates the centration of the achieved hyperopic ablation in this hyperopic eye the optical zone appears nasally decentered in reference to the pupillary image (dotted circle). It is nevertheless centered on the visual axis of this eye with a significant angle kappa.
Abbreviation: OD, right eye.

ie, "expansion" of the ablated mid peripheral cornea that has been ablated, resulting in progressive flattening of the steepened central cornea. We are currently using adjunctive collagen cross-linking techniques as a means of reducing and/or eliminating this effect.

Conclusion

Hyperopic and mixed astigmatism LASIK utilizing topography-guided 400 Hz Eye-Q excimer laser as well as the Intralase FS-60 and Alcon FS200 femtosecond lasers appear to be safe and very effective for correction of hyperopia and hyperopic astigmatism. The postoperative results at one and two years are impressive for correction of hyperopic and astigmatic refractive error and improvement in both corrected and uncorrected distance visual acuity, with minimal regression and need for enhancement.

Disclosure

This study was supported by an unrestricted fund from Alcon Laboratories, Fort Worth, TX.

References

1. Salz JJ, Stevens CA; LADARVision LASIK Hyperopia Study Group. LASIK correction of spherical hyperopia, hyperopic astigmatism, and mixed astigmatism with the LADARVision excimer laser system. *Ophthalmology*. 2002;109(9):1647–1656.
2. Lian J, Ye W, Zhou D, Wang K. Laser in situ keratomileusis for correction of hyperopia and hyperopic astigmatism with the Technolas 117C. *J Refract Surg*. 2002;18(4):435–438.
3. Carones F, Vigo L, Scandola E. Laser in situ keratomileusis for hyperopia and hyperopic and mixed astigmatism with LADARVision using 7 to 10-mm ablation diameters. *J Refract Surg*. 2003;19(5):548–554.
4. El-Agha MS, Bowman RW, Cavanagh D, McCulley JP. Comparison of photorefractive keratectomy and laser in situ keratomileusis for the treatment of compound hyperopic astigmatism. *J Cataract Refract Surg*. 2003;29(5):900–907.
5. Pineda-Fernandez A, Rueda L, Huang D, Nur J, Jaramillo J. Laser in situ keratomileusis for hyperopia and hyperopic astigmatism with the Nidek EC-5000 Excimer laser. *J Refract Surg*. 2001;17(6):670–675.
6. Goldberg DB. Comparison of myopes and hyperopes after laser in situ keratomileusis monovision. *J Cataract Refract Surg*. 2003;29(9):1695–1701.
7. Ditzen K, Fiedler J, Pieger S. Laser in situ keratomileusis for hyperopia and hyperopic astigmatism using the Meditec MEL 70 spot scanner. *J Refract Surg*. 2002;18(4):430–434.
8. Wygledowska-Promienska D, Zawojska I, Gierek-Ciaciura S. New generation of excimer laser – Asclepion Meditec MEL 70 G Scan. *Klin Oczna*. 2000;102:373–335; Polish.
9. Daush D. Landesz M. The Aesculap-Meditec laser: results from Germany. Laser correction for hyperopia. In: Salz JJ, editor. *Corneal Laser Surgery*. St Louis, MO: Mosby; 1995.
10. Sciscio A, Hull CC, Stephenson CG, Baldwin H, O'Brart D, Marshall J. Fourier analysis of induced irregular astigmatism. Photorefractive keratectomy versus laser in situ keratomileusis in a bilateral cohort of hyperopic patients. *J Cataract Refract Surg*. 2003;29(9):1709–1717.
11. Wang L, Koch DD. Anterior corneal optical aberrations induced by laser in situ keratomileusis for hyperopia. *J Cataract Refract Surg*. 2003;29(9):1702–1708.
12. Oshika T, Klyce SD, Applegate RA, Howland HC, El Danasoury MA. Comparison of corneal wavefront aberrations after photorefractive keratectomy and laser in situ keratomileusis. *Am J Ophthalmol*. 1999;127(1):1–7.
13. Kanellopoulos AJ, Conway J, Pe LH. LASIK for hyperopia with the WaveLight excimer laser. *J Refract Surg*. 2006;22(1):43–47.
14. Kanellopoulos AJ. Topography-guided custom retreatments in 27 symptomatic eyes. *J Refract Surg*. 2005;21(5):513–518.
15. Kanellopoulos AJ. Managing highly distorted corneas with topography-guided treatment. In: *ISRS/AAO 2007 Subspecialty Day/Refractive Surgery Syllabus. Section II: Ablation Strategies*. San Francisco, CA: American Academy of Ophthalmology; 2007.
16. Basmak H, Sahin A, Yildirim N, Papakostas TD, Kanellopoulos AJ. Measurement of angle kappa with synoptophore and Orbscan II in a normal population. *J Refract Surg*. 2007;23(5):456–460.
17. Gil-Cazorla R, Teus MA, de Benito-Llopis L, Mikropoulos DG. Femtosecond laser vs mechanical microkeratome for hyperopic laser in situ keratomileusis. *Am J Ophthalmol*. 2011;152(1):16–21.

Clinical Ophthalmology

Dovepress

Publish your work in this journal

Clinical Ophthalmology is an international, peer-reviewed journal covering all subspecialties within ophthalmology. Key topics include: Optometry; Visual science; Pharmacology and drug therapy in eye diseases; Basic Sciences; Primary and Secondary eye care; Patient Safety and Quality of Care Improvements. This journal is indexed on PubMed Central and CAS, and is the official journal of The Society of Clinical Ophthalmology (SCO). The manuscript management system is completely online and includes a very quick and fair peer-review system, which is all easy to use. Visit http://www.dovepress.com/testimonials.php to read real quotes from published authors.

Submit your manuscript here: http://www.dovepress.com/clinical-ophthalmology-journal

ORIGINAL RESEARCH

Placido disc vs Scheimpflug image derived topography-guided excimer laser surface normalization used combined with CXL (the Athens Protocol) in 181 progressive keratoconus cases.

A.John Kanellopoulos, M.D. [1,2]

George Asimellis, Ph.D. [1]

[1] Laservision.gr Eye Institute, Athens, Greece

[2] New York University School of Medicine, NY, USA

Correspondence: Professor A. John Kanellopoulos, MD

Laservision.gr Institute

17 Tsocha str. Athens, Greece Postal Code 11521

Tel +30 210 747 2777

Fax +30 210 747 2789

Email: ajk@brilliantvision.com

Acknowledgments/Disclosures

Dr. A J Kanellopoulos is a Consultant to Alcon/WaveLight.

Abstract

Purpose

To compare the efficacy of two alternative corneal topography data sources employed in the topography - guided excimer laser normalization, combined with CXL, in the management of keratoconus with the Athens Protocol (AP) procedure, namely a Placido-disk imaging device and a Scheimpflug imaging device.

Patients and methods

One hundred eighty-one (181) consecutive keratoconic cases subjected to the Athens Protocol procedure, between 2008 and 2011, were studied pre-operatively and 1, 3, 6, and 12-months postoperatively for visual acuity, keratometry, and anterior surface corneal indices. Two groups were formed, depending on the primary source for the topo-guided photoablation, namely a Placido disc, for group A (Placido), and a Scheimpflug rotating camera, for group B (Scheimpflug). The one-year changes in visual acuity, keratometric, and seven anterior-surface topometric indices were studied for both groups.

Results

The visual acuity changes, expressed as difference between post– minus the pre-operative corrected distance visual acuity were, for group A (Placido) +0.12 ± 0.20 (range +0.60 to -0.45), and for group B (Scheimpflug), +0.19 ± 0.20 (range +0.75 to –0.30), respectively.
For group A, K1 (flat keratometry) changed from 45.202 ± 3.782 diopters (D) to 43.022 ± 3.819, or a flattening of -2.18 D, and K2 (steep keratometry) changed from 48.670 ± 4.066 D to 45.865 ± 4.794 D, or a flattening of -2.805 D. Respectively, for group B, K1 (flat keratometry) changed from 46.213 ± 4.082 D to 43.190 ± 4.398 D, or a flattening of -3.023 D,

and K2 (steep keratometry) changed from 50.774 ± 5.210 to 46.380 ± 5.006 D, or a flattening of -4.394 D.

For group A, the value of the index of surface variance (ISV) was reduced to -5.07% and the value of the index of height decentration (IHD) to -26.81%. For group B, the value of the index of surface variance was reduced to -18.35% and the value of the index of height decentration to -39.03%, respectively. These value reductions indicate that the corneal surface became less irregular (ISV) and the 'cone' flatter and more central (IHD) in the post-operative assessment.

Conclusions

Of the two sources of primary corneal data, the Scheimpflug rotating camera (Oculyzer) for topography-guided normalization treatments with the WaveLight excimer laser platform, appear to provide statistically significant better improvement when compared to the Placido disk topographer (Vario Topolyzer). Overally, the Athens Protocol procedure, aiming to both arrest the keratoconus ectasia progression, as well as to improve corneal topometry and visual performance, demonstrates safe and notable refractive, keratometric and topometric results. The observed visual acuity changes, as well as keratometric flattening and topometric improvement are suggestive of the overall postoperative improvements.

Keywords

Athens Protocol; anterior surface Pentacam indices; keratoconus; cross-linking; WaveLight /Alcon excimer laser, EX500 excimer laser, topography-guided surface excimer ablation

Introduction

Keratoconus (KCN) is a degenerative bilateral, progressive, noninflammatory disorder characterized by ectasia, thinning and irregular topography. [1,2] It is associated with loss of visual acuity particularly in relation to corneal irregularity, [3,4] and usually is manifested asymmetrically between the two eyes of the same patient. [5,6]

Corneal collagen cross-linking (CXL) using riboflavin and ultraviolet-A (UVA) irradiation has become acceptable as a treatment option for eyes with progressive keratoconus. [7]

Laboratory data suggest that CXL employing riboflavin and UVA irradiation increases stromal collagen fibril diameter resulting in increased corneal biomechanical strength. [8] Several clinical reports indicate that CXL treatment results in arrest of ectasia progression, [7,9] in improvement of corneal keratometry, refraction and visual acuity, and in reduction of higher-order aberrations; the post-operative complications are infrequent. [7] Our team has introduced several variations and applications with CXL. [10,11]

We have also introduced and reported in extent, in conjunction with the CXL treatment, sequential partial topography-guided photorefractive keratectomy (PRK), [12] which provides a promising approach for further improvement of the topometric and refractive outcomes [13] with good long-term stability. [14,15] Further, we introduced and have extensively reported [16-20] the combination of (a) excimer-laser removal of the top 50 μm of the epithelium, (b) partial topography-guided excimer ablation, limited to maximum of 50 μm stromal tissue removal, followed in the same session by (c) immediate high-fluence UVA radiation (5,6 and 10 mW/cm^2), short duration (18, 15, 10΄) CXL, in a procedure known as the Athens Protocol (AP). [21, 22] The surgical technique of the Athens Protocol has been described with detail previously. [23]

This study aims to compare the efficacy of two alternative corneal topography data sources employed in the topography - guided part of the procedure with the WaveLight/Alcon excimer laser platform (Alcon, Ft. Worth, TX), specifically, a Placido-disk imaging device and a Scheimpflug imaging device, by analysis of long term refractive, topometric and visual rehabilitation changes.

Materials and methods

This clinical series study received approval by the Ethics Committee of our Institution, adherent to the tenets of the Declaration of Helsinki. Informed consent was obtained from each subject at the time of the Athens Protocol intervention or the first clinical visit. The study was conducted in our clinical practice on patients before the AP procedure and/or scheduled clinical visits.

Patient inclusion criteria

The study group consisted of one hundred eighty-one (181) consecutive keratoconic cases subjected to the Athens Protocol procedure, between 2008 and 2011. In all procedures - performed by the same surgeon (AJK)- the epithelial excimer-laser removal, as well as the topography-guided excimer-laser ablation was provided by the Alcon/WaveLight 400 Hz Eye-Q [24] or the 500 Hz EX500 excimer lasers. [25,26]

For a patient to be considered for the AP procedure, the following criteria were met: clinical diagnosis of progressive keratoconus, minimum age of 18 years, and minimum corneal thickness of 300 μm. No patient with systemic disease, previous corneal surgery, history of chemical injury or delayed epithelial healing, and pregnancy or lactation (for the female patients) were considered for the procedure. All patients included in the study completed an uneventful Athens Protocol procedure using the KXL CXL device (Avedro, Waltham, MA), and were presented to our institution for at least one-year follow-up monitoring.

Depending on the imaging source for the topography-guided partial photoablation, the following two groups were formed: Group A (nA = 54 eyes), in which the primary topography data were provided by a Placido-disk imaging device, and Group B (nB = 127 eyes), in which the primary topography data were provided by a Scheimpflug imaging device.

Imaging and measurement

The Placido-disk diagnostic device employed was the Alcon/WaveLight® Allegro Topolyzer™ Vario™ (WaveLight AG, Erlagen, Germany). The Topolyzer is a wide-cone corneal topographic Placido system with 22 concentric rings for the detection of up to 22,000 elevation points. The Placido-ring image is referenced to the corneal apex and locates the pupil center and the limbus. An automatic measuring release ensures that the image centration has a peripheral standard deviation (StDev) of ± 4 μm. The embedded pupil-recognition software can measure pupil centroid shift, allowing centration of the subsequent laser ablation according to the patient's visual needs. The Athens Protocol -based on topographic data from the Topolyzer (Group A) is thus referred to as 'Placido-disc guided', or simply, 'Placido' in which for each eye, eight acquisitions averaged for consistency, are employed.

The Scheimpflug diagnostic device employed was the Alcon/WaveLight® Oculyzer™ II. The Oculyzer is a high-resolution Pentacam camera (Oculus Optikgeräte GmbH, Wetzlar, Germany) [27] which is incorporated into the Alcon/WaveLight Refractive Suite. [25] The integrated, rotating Scheimpflug camera acquires up to 50 images in real-time measurement. The Athens protocol was based on data from the Oculyzer (Group B) is thus referred to as 'Scheimpflug-guided', or simply 'Scheimpflug', in which for each eye, four acquisitions, averaged for consistency, are employed.

Post-operative follow-up assessment was performed by means of subjective refraction, best spectacle Corrected Distance Visual Acuity (CDVA) measurement with this refraction, and slit-lamp biomicroscopy, as well as anterior segment optical coherence tomography (OCT) imaging for clinical signs of corneal CXL. [15]

Anterior-surface topographic indices

To measure and monitor the induced topographic changes in keratometric refraction and topographic geometry, quantitative post-operative assessment (measured both pre-operatively and at 1, 3, 6, and 12 months postoperatively) was performed by the Oculyzer II, obtained and processed via the Oculyzer Examination Software (Version 1.17r47). For each eye, four consecutive measurements were obtained and processed to test for data repeatability (including topographic, tomographic, and pachymetric mapping). [21]

To this aim, in addition to keratometric measurements, specific anterior-surface indices when used in conjunction with the Pentacam camera analysis were studied, developed for the grading and classification based on the Amsler & Krumeich keratoconus stages, [29] as well as the post-operative assessment. [30-36]

These indices are the following: index of surface variance (ISV), an expression of corneal surface curvature irregularity; the index of vertical asymmetry (IVA), a measure of the difference between superior and inferior corneal curvature; the keratoconus index (KI); the central keratoconus index (CKI); the index of height asymmetry (IHA), a measurement similar to the IVA but based on corneal elevation; the index of height decentration (IHD), calculated with Fourier analysis of corneal height to quantify the degree of vertical decentration; and the minimum radius of curvature (Rmin), a measurement of the smallest radius of curvature of the cornea (ie, the maximum corneal steepness). [37] In the present work, the 12-month post-operative data were studied in comparison of the pre-operative respective data.

Linear regression analysis was performed to seek possible correlations between changes of these indices as well as visual rehabilitation. Descriptive and comparative statistics, analysis of variance between keratoconus stage subgroups and linear regression were performed with statistics tools provided by Minitab version 1.6.1 (MiniTab Ltd., Coventry, UK) and Origin Lab version 9 (OriginLab Corp, Northampton, MA). Paired analysis p-values less than 0.05 were considered indication of statistically significant results.

Results

Subjects' ages for group A at the time of the AP operation was (average ± standard deviation) 31.5 ± 7.9 years, (min 19, max 57), while for group B, 33.3 ± 7.3 years (min 21, max 57). Gender specifics for group A were 16 female and 38 male patients, while for group B, 42 female and 85 male. There is a preponderance towards male population, which is consistent with our clinical experience [15] and keratoconus incidence studies. [38] In group A, 25 eyes were right (OD) and 29 left (OS), while in group B, 69 eyes were right and 58 left.

Visual Acuity Changes

Preoperative average CDVA (expressed decimally) was, for group A: (average ± standard deviation) 0.65 ± 0.23, range (max-min 1.00 to 0.10), and for group B: 0.63 ± 0.24 (range 1.00 to 0.10) (Table 1). The visual acuity changes, expressed as difference between post– minus the pre-operative CDVA were, for group A, +0.12 ± 0.20 (range +0.60 to -0.45), and for group B, +0.19 ± 0.20 (range +0.75 to –0.30), respectively.

Figures 1 illustrate the above data in the form of box plots, showing median level (indicated by ⊗), average symbol (⊕), 95% median confidence range box, and interquartile intervals range box. As shown in Figure 1b, the 95% median confidence range box shows that in both groups, 95% the eyes had positive change (stable or better) in visual acuity.

Keratometric and topographic indices distribution

Average, standard deviation (StDev), maximum (Max) and minimum (Min) anterior and posterior corneal surface keratometry and topometric indices, as measured in the 8 mm zone for both groups, pre- and 12-months post-operatively are presented in Table 2. Box plot describing induced changes (comparison pre- to post-operative values) for anterior K1 flat (top) and steep K2 (bottom) keratometry (in diopters, D) for group A and B are presented in Figures 2a and b, respectively. The resulting induced changes for all seven anterior surface indices for the two groups are reported in Table 3.

The anterior-surface keratometry had the following averaged changes (defined as the post-average operative value with regard to the respective preoperative value, from the data in table 2): for group A, K1 (flat) changed from 45.202 ± 3.782 diopters (D) to 43.022 ± 3.819, or a change of -2.18 D, and K2 (steep) changed from 48.670 ± 4.066 D to 45.865 ± 4.794 D, or a change of -2.805 D. Respectively, for group B, K1 (flat) changed from 46.213 ± 4.082 D to 43.190 ± 4.398 D, or a change of -3.023 D, and K2 (steep) changed from 50.774 ± 5.210 to 46.380 ± 5.006 D, or a change of -4.394 D.

Anterior-surface topographic index and keratoconus stages correlation

All eyes in both groups were pre-operatively classified by the Oculus software to keratoconus Amsler & Krumeich severity index stages (-, KC1, KC1-2, KC2, KC2-3, KC3, KC3-4, and KC4).

We pursued correlations between all of the seven anterior-surface topographic images with the above grading stages. The correlation between the derived keratoconus severity index and the seven anterior-surface topographic indices is illustrated in the form of box plots in Figures 3. The result was that the best correlates with the keratoconus stage classification were the ISV (with the exception of the highest stage KC4, all other P-values were < 0.001, as

seen in Table 4), and by the IHD (with the exception of the lowest stage KC1, all other P-values were < 0.001).

We also conducted index repeatability measurement study, and expressed the measured repeatability as the relative (%) change between four consecutive measurements of the same eye (lower values indicating better repeatability). The results indicated that the indices ISV and IHD were among the best performers, having an average repeatability of 2.77% ± 1.32% for the ISV, and 4.67% ± 1.62%, for the IHD index, respectively.

Anterior-surface topographic index post-operative changes

Based on the above mentioned results, we thus chose to follow these two indices, ISV and IHD, as reliable indicators of anterior-surface changes induced by the AP procedure. By their respective definitions, a change towards a lower value (negative change) is indicative of a trend towards a more normal corneal keratometry and topography. [31]

The AP-induced changes, expressed as difference of the 12-month post-operative minus the respective pre-operative values are illustrated in figures 4 (ISV changes) and figures 5 (IHD changes). The indices ISV and IHD had the following relative changes (defined as % of the change of the parameter with regard to the respective preoperative value), as shown in table 3: for group A, ISV was reduced to -5.07% and IHD to -26.81%, and for group B, ISV was reduced to -18.35% and IHD to -39.03%, respectively. This negative change is indicative of corneal surface becoming less irregular (ISV) and the 'cone' becoming more central (IHD) in the post-operative assessment.

Comparison of Placido-disk and Scheimpflug camera imaging for the topo-guided ablation

The above data, ie the changes in visual acuity, keratometry, as well as the anterior surface topometric indices, indicate that there exists a differential in the outcomes when comparing the two groups, group A (Placido disk) and group B (Scheimpflug camera).

To further expand our investigation we formed two subgroups within each group, based on the criterion of pre-operative value of IHD. The distinction was made by arbitrarily defining 'low IHD' if less or equal to 0.09, referring to a more centered keratoconus cone, and 'high IHD' if larger than 0.09, referring to a more decentered cone. Then, the following subgroups were formed: group A1, Placido Low, consisting of nAL = 30 eyes; group A2, Placido High, consisting of nAH = 24 eyes; group B1, Scheimpflug Low, consisting of nBL = 65 eyes; and group B2, Scheimpflug High, consisting of nBH = 64 eyes. Consequently we investigated within each such subgroup the induced AP changes in the IHD index. For group A1, the relative (%) change in ISV was -4.61% and in IHD -22.10% and for group A2, the relative (%) change in ISV was -5.35% and in IHD -29.05%. For group B1, the relative (%) change in ISV was -13.54% and in IHD -32.82% and for group B2, the relative (%) change in ISV was -20.36% and in IHD -41.19%. The results are presented in the form of box plots in Figure 6, and are tabulated in Table 5.

Discussion

For the clinical assessment and evaluation of keratoconus and the monitoring of induced postoperative potential improvement due to CXL procedures, the current options of the clinical investigator includes a multitude of diagnostic devices. Corneal pachymetry [39,40] and cornea biomechanical properties analysis [41] can also be very significant in the keratoconus assessment, although the long-standing standard for evaluating keratoconus and treatment results has been anterior surface topometry and topography. [42]

It has been known that CXL alone results in a change in corneal pachymetry, which may not be accurately depicted by the Scheimpflug imaging due to the principle of operation, namely densitometry. In addition the –partial- photoablation part of the AP procedure reduces corneal thickness, and thus any classification criteria scheme which includes corneal pachymetry may be insufficient for the post-operative assessment. Particularly after

treatment (eg CXL), changes in the anterior surface may provide a more pertinent analysis of the changes induced by the procedure. [43,44]

Our clinical observation, which is also confirmed by other researchers, [45] has been that postoperatively, the short-term (particularly during the first 6-month period) refractive, topometric, and pachymetric results [46] can be described as being 'in continuous change', with progressive improvement towards the one-year assessment, and possibly further on. Because of this, we chose to select and analyze the one-year interval results as a common reference to what we subsequently call 'postoperative data'. In this study thus, we evaluated the one-year postoperative changes induced by the AP procedure in visual acuity, keratometry, and seven anterior surface topographic indices, and investigated associations with visual acuity outcomes.

Our results indicate that the Rmin (minimum radius of curvature), which is defined as the inverse of corneal steepness, was increased postoperatively in agreement with the decrease of anterior surface keratometry [47,48] (Table 2). As such, the improved observed one-year improvement in CDVA (Table 1 and Figure 1) can be justified, as the anterior corneal surface attains a more optically manageable refractive shape. In all other six topographic indices, their values were reduced in comparison to the respective preoperative values, indicating corneal surface improvement. The noted postoperative reduction of some of these indices has been reported only recently. [31] These changes are all indicative of corneal topography improvement, (ie reduction of irregularity, cone becoming less steep and more central) in agreement with other studies. [31, 41] It appears thus that the option to quantitatively assess CXL postoperative changes with the ISV and IHD topometric indices may be proven very helpful in the clinical practice.

Topography-guided ablation for keratoconus: which is the best image source for guidance?

Our study indicates that the outcomes of the Athens Protocol employed for keratoconus stabilization and visual rehabilitation appear to be better when using the Scheimpflug driven topography data. Based on our analysis, the group B, whose primary topographic data were provided by the Oculyzer II, a Scheimpflug rotating camera, when compared to the group A, whose primary topographic data were provided by the Vario Topolyzer, a Placido topographer, presented a more drastic reduction in keratometry, as well as the two anterior-surface topographic indices with the strongest correlation with keratoconus grading, namely the indices ISV and IHD.

This study evaluates a very large number of cases over an extended amount of time, when compared to the current peer-reviewed literature. The difference in absolute numbers between group A (Placido-disc guided) of 54 cases, and group B (Scheimpflug tomography-guided) of 127 is due to the early results suggesting that group B was of higher efficacy and thus, discontinuing recruitment of group A patients. Although different, these numbers and follow-up is still quite large and permits sensitive statistical analysis with confident conclusion of the differential in post-operative efficacy.

This change is more pronounced in the pre-operative more irregular and more decentrated anterior surfaces (subgroups A2 and B2), reaching up to a -41% reduction in the index of height decentration for group B2.

The above findings may be explained by the principles of operation of the corresponding diagnostic devices. Specifically, the Placido-disk imaging devices, despite providing a single, snap-shot measurement, are more suitable for peripheral cornea measurements, and have lower information reliability at the corneal center, in addition to being susceptible to error

due to abrupt corneal height changes. Specifically, Placido disc imaging cannot clearly differentiate between abrupt flattening to abrupt steepening changes, just measures curvature changes. This potential bias of measurement may be one, or the main, reason of the clinical efficacy difference in our data. On the other hand, the Scheimpflug imaging camera rotating measurement process, despite being sequential, captures images with a fine meshed dot matrix in the center, providing high-resolution data of absolute elevation from the large corneal area imaged. The potential bias here is the eyelid and eyelash interference in the image quality, as well as the potential bias of thickness measurement attributed to arcus senilis changes of the peripheral cornea. All Scheimpflug images used in our treatments are carefully screened in order to exclude these potential biases.

Conclusions

Topography-guided normalization of extreme cornea irregularity such as keratoconus, coupled with CXL appears to be achieved with statistically-different higher efficacy when the Scheimpflug rotating camera (Oculyzer) is used with the WaveLight excimer laser platform. It appears to provide statistically significant better refractive, topometric, and visual rehabilitation improvement when compared to the Placido disk (Topolyzer) topography-driven normalization and CXL treatments. This Athens Protocol procedure, aiming to both arrest the keratoconus ectasia progression, as well as to improve anterior corneal normality and topometry and visual performance, demonstrates good safety record with either platform and very effective refractive, keratometric and topometric results.

.

Tables

Table 1

Best spectacle corrected distance visual acuity (CDVA) data, expressed decimally: Pre-operative, 12-month post-operative, and change (gain/loss), expressed as the difference of post minus the pre-operative CDVA.

	Pre-Operative		Post-Operative		Change (gain/loss)	
	Group A (Placido)	Group B (Scheimpflug)	Group A (Placido)	Group B (Scheimpflug)	Group A (Placido)	Group B (Scheimpflug)
average	0.65	0.63	0.77	0.82	0.12	0.19
StDev	± 0.23	± 0.24	± 0.19	± 0.19	± 0.20	± 0.20
Max	1.00	1.00	1.10	1.20	0.60	0.75
Min	0.00	0.00	0.30	0.30	-0.45	-0.30
Shapiro-Wilk normality test p value	> 0.100	0.049	> 0.100	< 0.010	> 0.100	0.054

Table 2

Average, standard deviation (StDev), maximum (Max) and minimum (Min) anterior and posterior corneal keratometry and topometric indices, as measured in the 8 mm zone for both groups, pre- and 12-months post-operatively. Abbreviations: ISV, Index of Surface Variance; IVA, Index of Vertical Asymmetry; KI, Keratoconus Index; CKI, Central Keratoconus Index; IHA, Index of Height Asymmetry; IHD, Index of Height Decentration; Rmin, smallest sagittal curvature.

Group A	**Placido**	**Pre-Op**					**Post-Op**			
		average	stdev	max	min		average	stdev	max	min
Anterior Surface	K1 (flat) (D)	45.20	± 3.78	52.1	33.7		43.02	± 3.82	52.6	31.8
	K2 (steep) (D)	48.67	± 4.07	59.2	42.1		45.86	± 4.79	59.8	34.6
	Km (mean) (D)	46.88	± 3.60	54.6	41.3		44.37	± 4.14	54.5	33.1
Posterior Surface	K1 (flat) (D)	-6.44	± 0.78	-4.6	-8.0		-6.39	± 0.86	-4.8	-8.5
	K2 (steep) (D)	-7.28	± 0.84	-5.9	-9.4		-7.40	± 0.91	-5.8	-10.1
	Km (mean) (D)	-6.82	± 0.74	-5.5	-8.6		-6.85	± 0.82	-5.6	-9.2
Anterior Surface Indices	ISV	91.33	± 42.59	187	14		86.70	± 43.91	190	14
(in 8mm zone)	IVA	1.06	± 0.54	2.52	0.09		1.00	± 0.59	2.69	0.13
	KI	1.25	± 0.15	1.72	1.02		1.21	± 0.17	1.66	0.93
	CKI	1.05	± 0.05	1.30	0.98		1.04	± 0.06	1.16	0.86
	IHA	26.19	± 19.80	84	0.60		22.20	± 18.37	75.1	3.3
	IHD	0.087	± 0.051	0.201	0.007		0.064	± 0.043	0.163	0.005
	Rmin (mm)	6.35	± 0.70	7.73	5.03		6.69	± 0.71	7.93	4.96

Group B	**Scheimpflug**	**Pre-Op**					**Post-Op**			
		average	stdev	max	min		average	stdev	max	min
Anterior Surface	K1 (flat) (D)	46.21	± 4.08	60.7	37.6		43.19	± 4.40	55.3	30.5
	K2 (steep) (D)	50.77	± 5.21	71.7	42.6		46.38	± 5.01	59.5	35.7
	Km (mean) (D)	48.36	± 4.44	65.7	40.7		44.71	± 4.58	57.3	32.9
Posterior Surface	K1 (flat) (D)	-6.58	± 0.83	-4.6	-9.0		-6.52	± 0.96	-3.3	-9.8
	K2 (steep) (D)	-7.66	± 1.08	-5.8	-10.9		-7.68	± 1.13	-5.6	-11
	Km (mean) (D)	-7.07	± 0.90	-5.1	-9.8		-7.04	± 0.98	-4.6	-10.3
Anterior-surface Indices	ISV	98.14	± 45.32	208	18		80.13	± 35.98	169	15
(in 8mm zone)	IVA	1.05	± 0.51	2.45	0.17		0.87	± 0.46	2.42	0.1
	KI	1.27	± 0.16	1.80	0.97		1.19	± 0.15	1.56	0.86
	CKI	1.05	± 0.06	1.30	0.90		1.02	± 0.05	1.16	0.87
	IHA	30.95	± 20.88	88.7	0.3		23.80	± 17.36	96.3	0.1
	IHD	0.09	± 0.05	0.26	0.01		0.06	± 0.03	0.172	0.001
	Rmin (mm)	6.07	± 0.79	7.61	4.20		6.65	± 0.66	7.88	5.12

Table 3

Induced changes for the seven anterior-surface indices for the two groups. Average change is defined as post-operative minus the pre-operative value). Relative change is defined as % of the average change of the parameter with regard to the respective preoperative value.

	ISV	IVA	KI	CKI	IHA	IHD	Rmin (mm)
	Group A (Placido)						
relative change	-5.07%	-5.65%	-3.20%	-1.42%	-15.24%	-26.81%	2.18%
average change	-4.630	-0.060	-0.040	-0.015	-3.991	-0.023	0.139
stdev	± 16.617	± 0.225	± 0.066	± 0.055	± 21.003	± 0.027	± 0.263
max	29	0.45	0.07	0.06	40.6	0.023	1.31
min	-50	-0.74	-0.23	-0.27	-57.5	-0.102	-0.28
	Group B (Scheimpflug)						
relative change	-18.36%	-16.64%	-6.24%	-3.24%	-23.10%	-39.03%	9.64%
average change	-18.016	-0.175	-0.079	-0.034	-7.150	-0.035	0.585
stdev	± 20.687	± 0.253	± 0.073	± 0.042	± 17.087	± 0.036	± 0.409
max	38	0.42	0.08	0.06	37.7	0.017	1.93
min	-83	-0.95	-0.43	-0.22	-65.1	-0.213	-0.22

Table 4

Two-sample t-test results, not assuming equal variances, between the keratoconus grading subgroups (KC1, KC1-2, KC2, KC2-3, KC3, KC3-4, KC4) for the ISV and IHD topometric indices as measured pre-operatively. Abbreviations: ISV, index of surface variance; IHD, index of height decentration; CI, Confidence interval.

ISV	Estimate for difference:	95% CI for difference:	P-Value
K1 vs K1-2	10.31	(7.35, 13.27)	<0.001
K1-2 vs K2	21.84	(17.87, 25.82)	<0.001
K2 vs K2-3	21.02	(17.02, 25.03)	<0.001
K2-3 vs K3	20.3	(16.88, 23.72)	<0.001
K3 vs K3-4	43.7	(37.79, 49.62)	<0.001
K3-4 vs K4	61	(14.1, 107.8)	0.026

IHD	Estimate for difference:	95% CI for difference:	P-Value
K1 vs K1-2	0.01255	(0.00474, 0.02035)	0.003
K1-2 vs K2	0.02411	(0.01522, 0.03300)	<0.001
K2 vs K2-3	0.02012	(0.01038, 0.02985)	<0.001
K2-3 vs K3	0.01856	(0.00836, 0.02876)	0.001
K3 vs K3-4	0.04487	(0.03165, 0.05808)	<0.001
K3-4 vs K4	0.0888	(0.0610, 0.1166)	<0.001

Table 5

Induced changes for the ISV and IHD indices for the four sub groups. Average change is derived from the post-operative minus the pre-operative value in each case. Relative change is defined as % of the average change of the parameter with regard to the respective preoperative value. Abbreviations: ISV, index of surface variance; IHD, index of height decentration

	ISV	IHD		ISV	IHD
	Group A1 – Placido Low			**Group A2 – Placido High**	
relative	-4.61%	-22.10%		-5.35%	-29.05%
average	-2.900	-0.011		-6.792	-0.038
stdev	± 17.010	± 0.020		± 16.208	± 0.026
max	29	0.023		23	0.013
min	-50	-0.054		-36	-0.102
	Group B1 – Scheimpflug Low			**Group B2 – Scheimpflug High**	
relative	-13.54%	-32.82%		-20.36%	-41.19%
average	-8.908	-0.016		-26.750	-0.054
stdev	± 18.339	± 0.020		± 18.968	± 0.037
max	38	0.014		13	0.017
min	-48	-0.074		-83	-0.213

Figures **Figure 1**

Box plots of CDVA (expressed decimally): (Top) Pre-operative, and post-operative values for both groups. (Bottom) Gain/loss expressed as difference between post- minus pre-operative CDVA. Box plots are showing median level (indicated by ⊗), average symbol (⊕), 95% median confidence range box (black borderline boxes), and interquartile intervals range box (red borderline boxes).

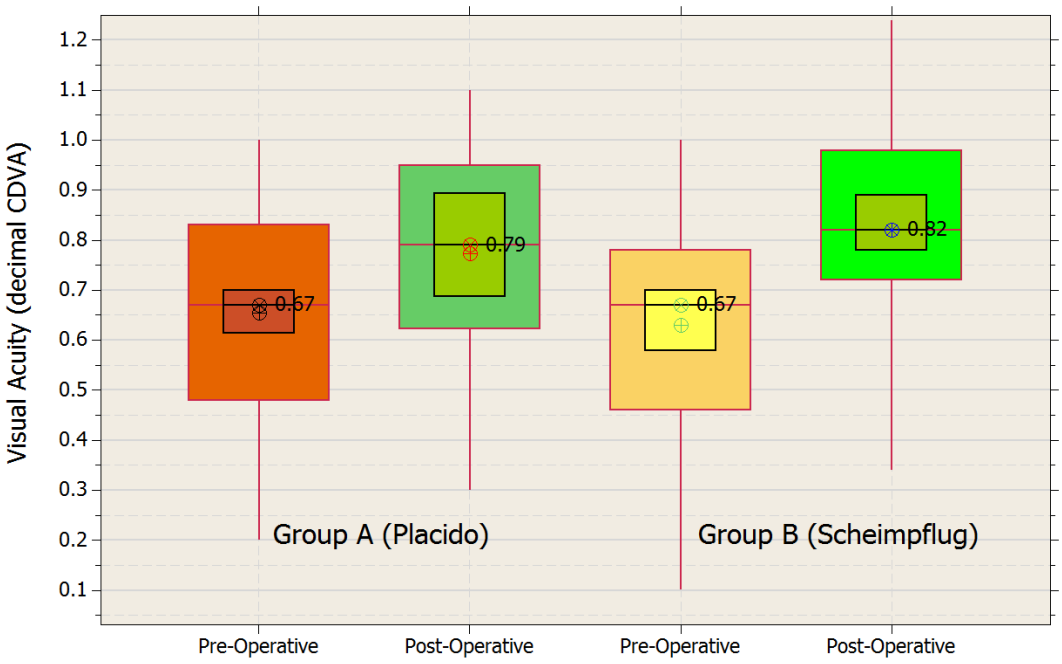

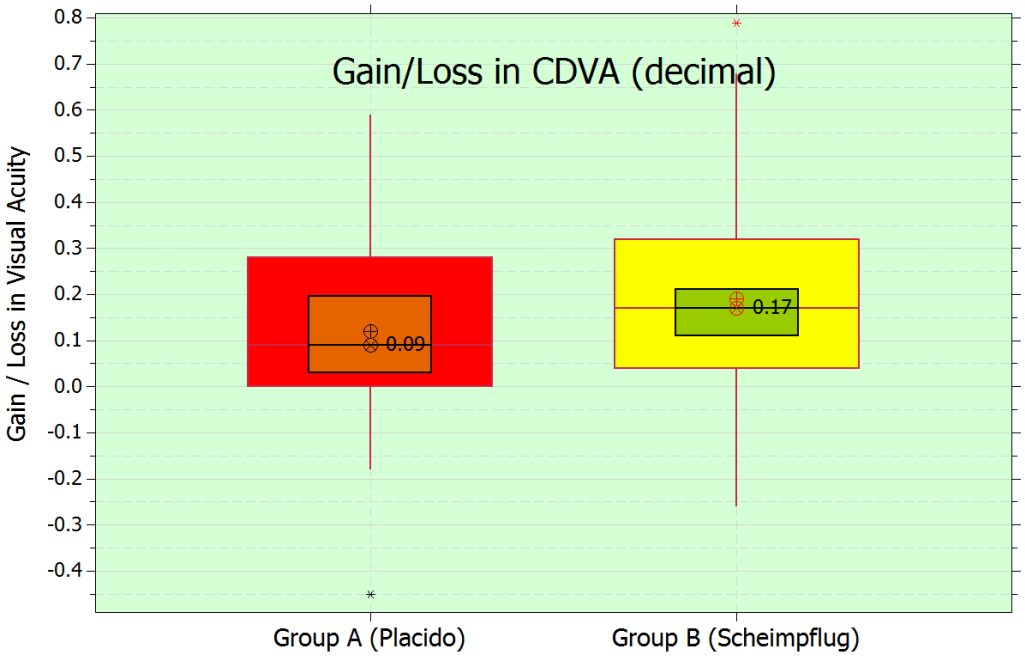

Figure 2a

Box plot describing induced changes (comparison pre- to post-operative values) for anterior flat (top) and steep (bottom) keratometry (in diopters, D) for group A (Placido). Median level is indicated by ⊗, average by ⊕, the 95% median confidence range box by the red borderline, and the interquartile intervals range box by the black borderline.

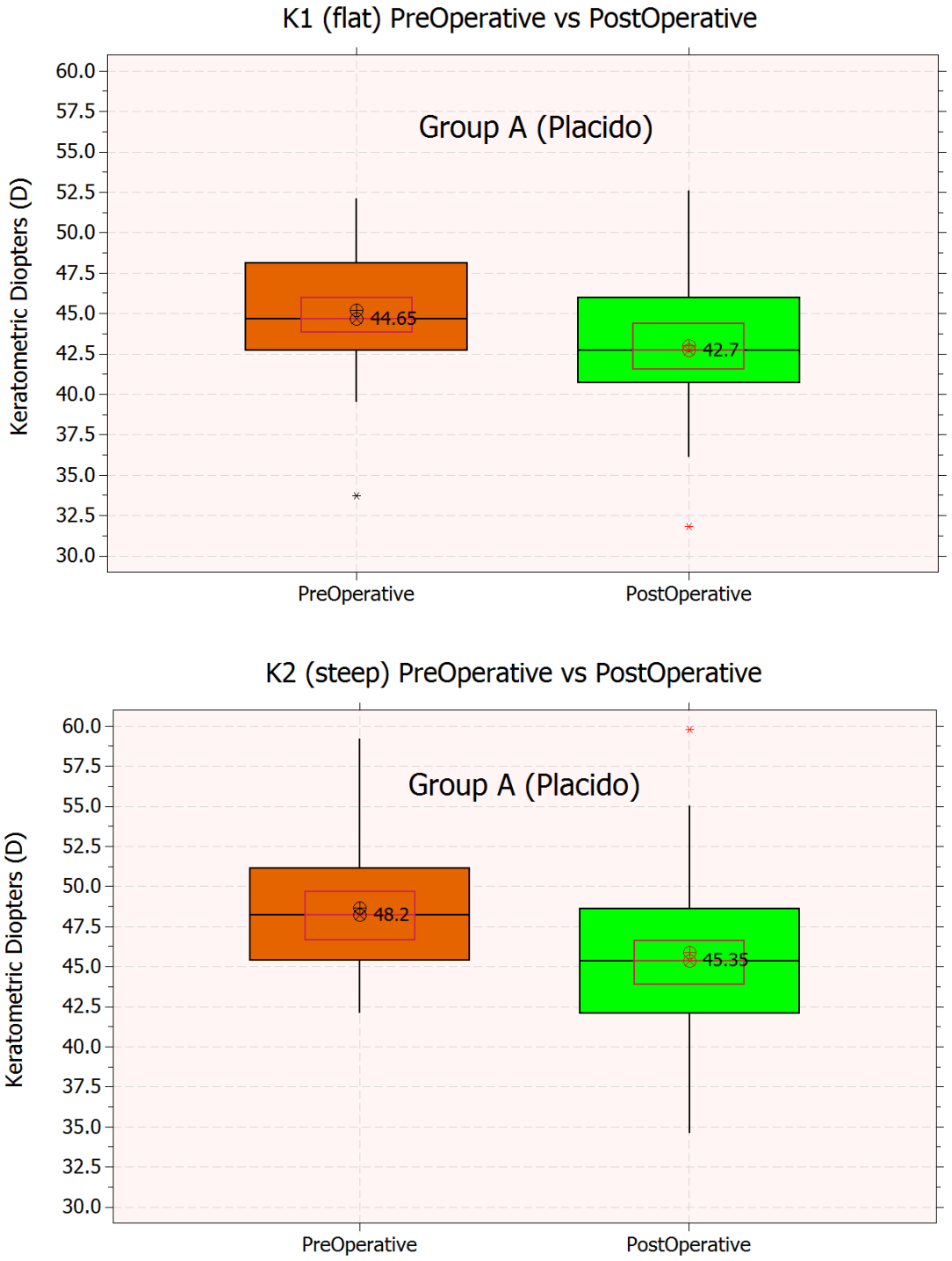

Figure 2b

Box plot describing induced changes (comparison pre- to post-operative values) for anterior flat (top) and steep (bottom) keratometry (in diopters, D) for group B (Scheimpflug). Median level is indicated by ⊗, average by ⊕, the 95% median confidence range box by the red borderline, and the interquartile intervals range box by the black borderline.

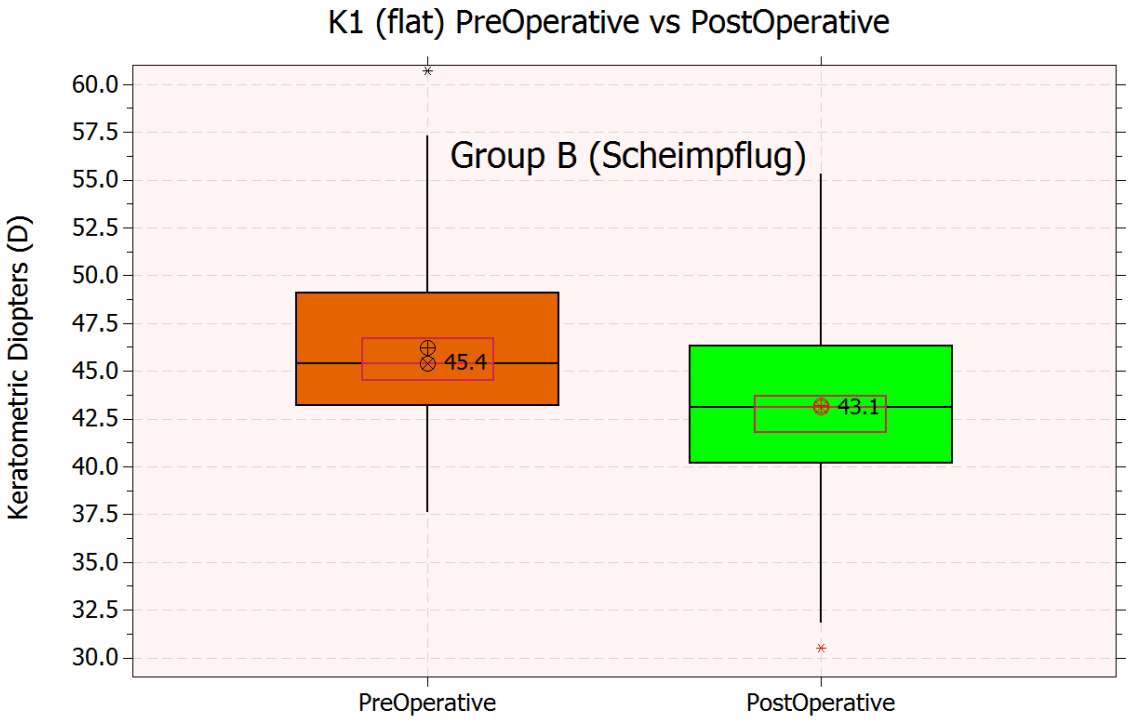

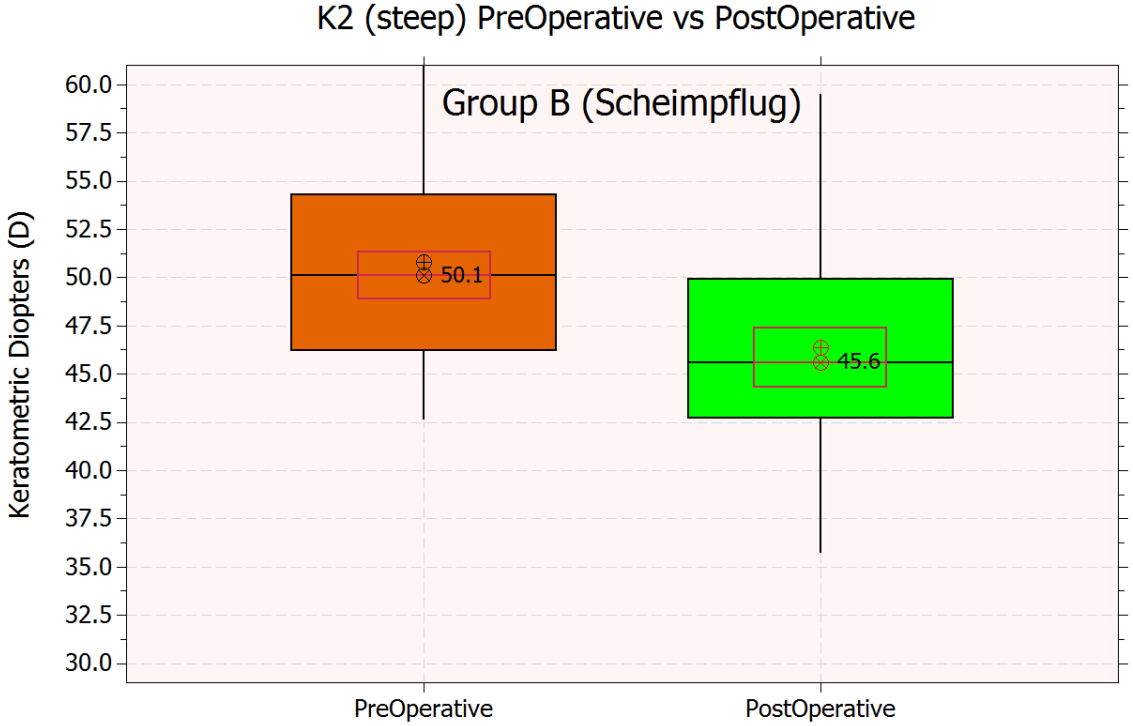

Figure 3

Top, box plot of pre-operative ISV (Index of Surface Variance) and bottom, preoperative IHD (Index of Height Decentration) vs keratoconus grading, as produced by the Oculyzer software. Median level is indicated by ⊗, average by ⊕, the 95% median confidence range box by the lack borderline, and the interquartile intervals range box by the red borderline.

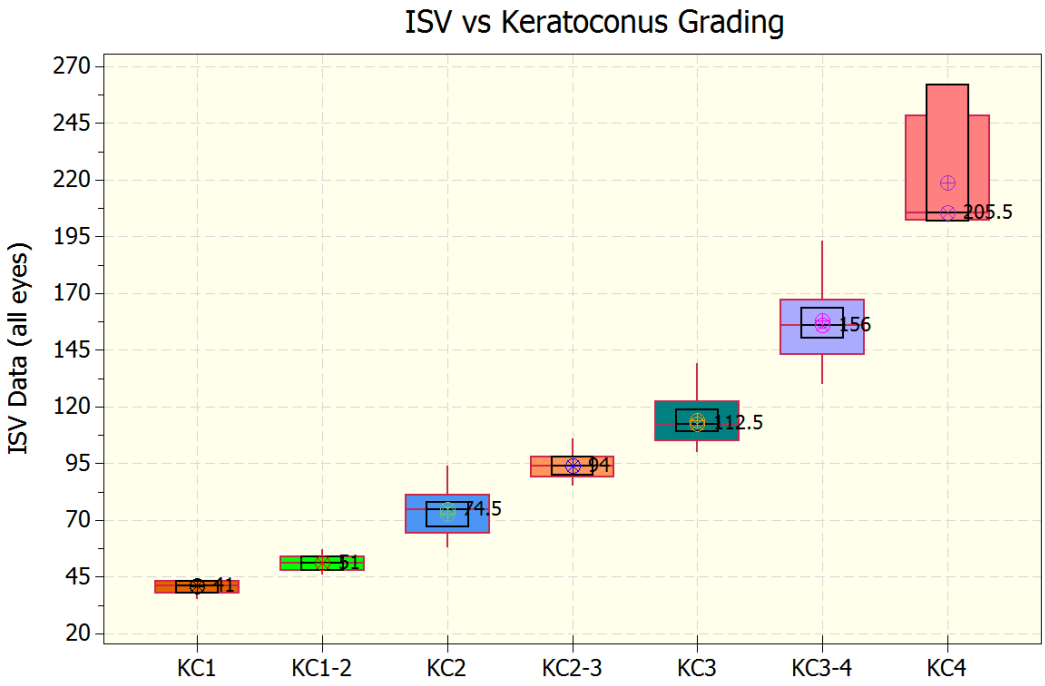

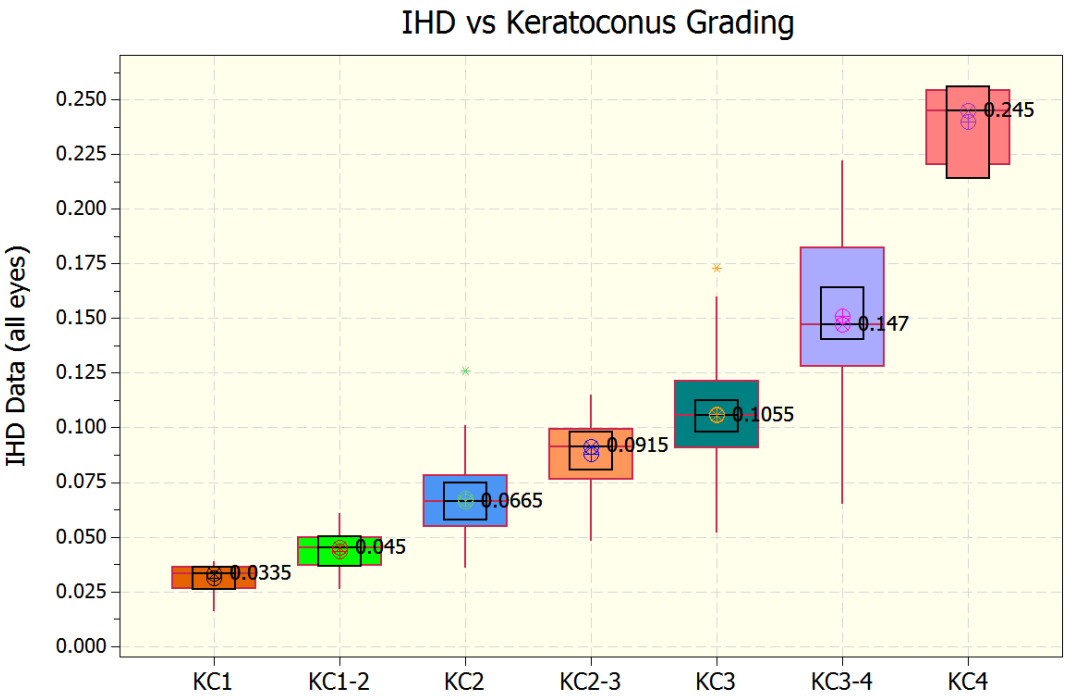

Figure 4

Box plot describing induced changes (comparison of pre to post-operative values) for the index of surface variance (ISV) for the two groups: top, group A, Placido, and bottom, group B, Scheimpflug. Median level is indicated by ⊗, average by ⊕, the 95% median confidence range box by the red borderline, and the interquartile intervals range box by the black borderline.

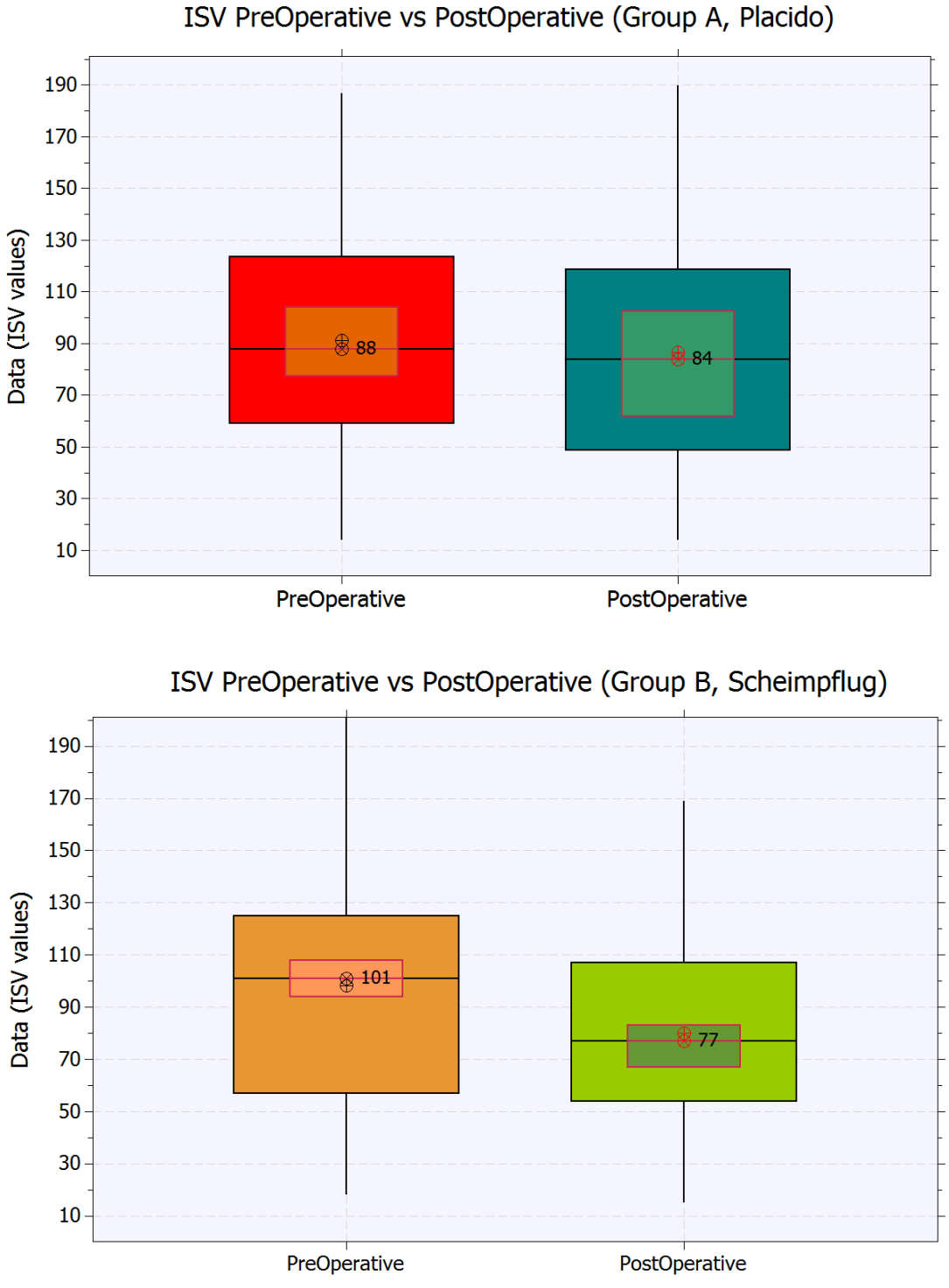

Figure 5

Box plot describing induced changes (comparison of pre to post-operative values) for the index of height decentration (IHD) for the two groups: top, group A, Placido, and bottom, group B, Scheimpflug. Median level is indicated by ⊗, average by ⊕, the 95% median confidence range box by the red borderline, and the interquartile intervals range box by the black borderline.

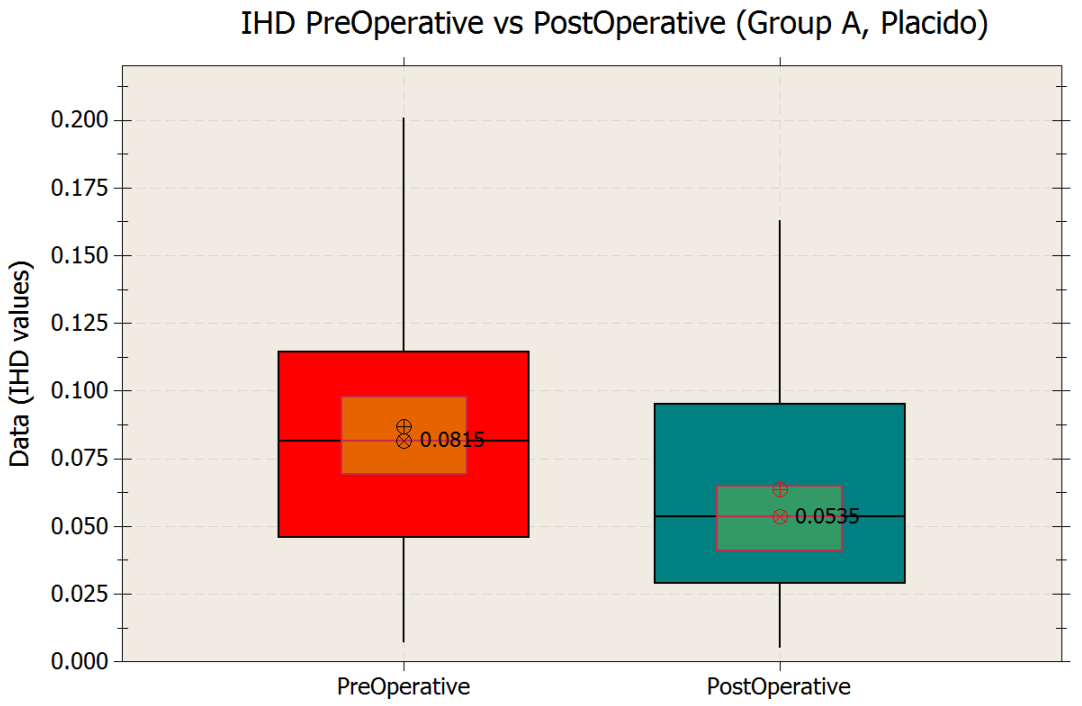

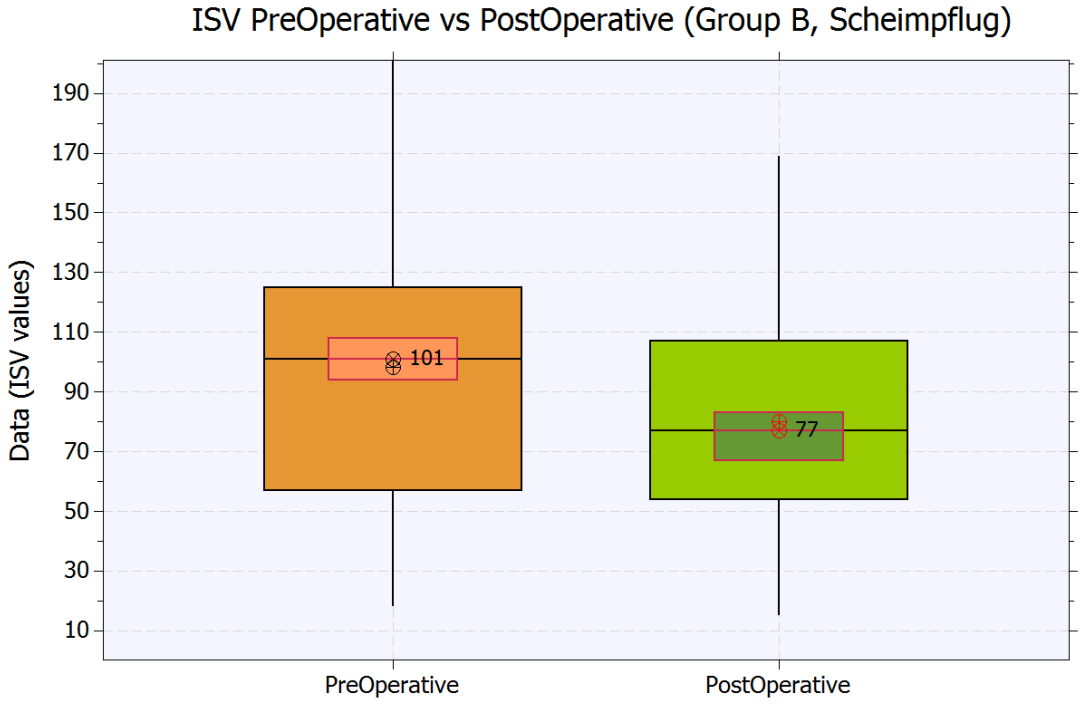

Figure 6a

Box plot describing induced changes (comparison of pre to post-operative values) for the index of height decentration (IHD) for the subgroups: top, group A1 – Placido Low, indicating less affected keratoconic eyes, and bottom, group A2 – Placido High, indicating more affected keratoconic eyes.

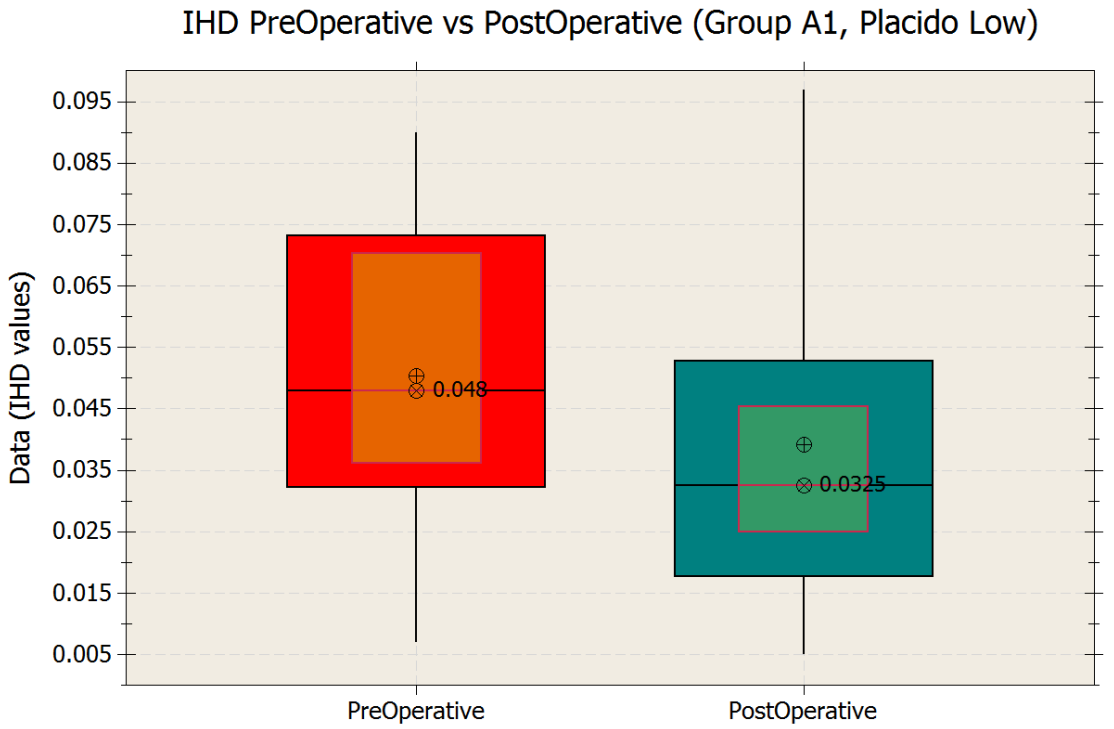

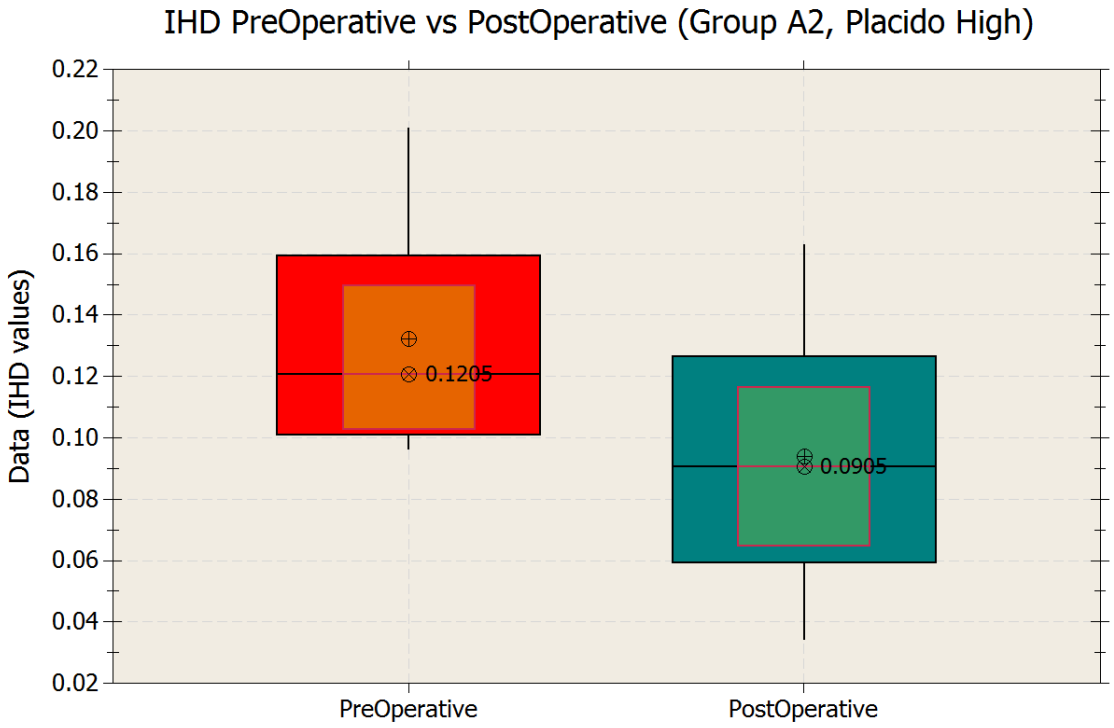

Figure 6b

Box plot describing induced changes (comparison of pre to post-operative values) for the index of height decentration (IHD) for the subgroups: top, group B1 – Scheimpflug Low, indicating less affected keratoconic eyes, and bottom, group B2 – Scheimpflug High, indicating more affected keratoconic eyes.

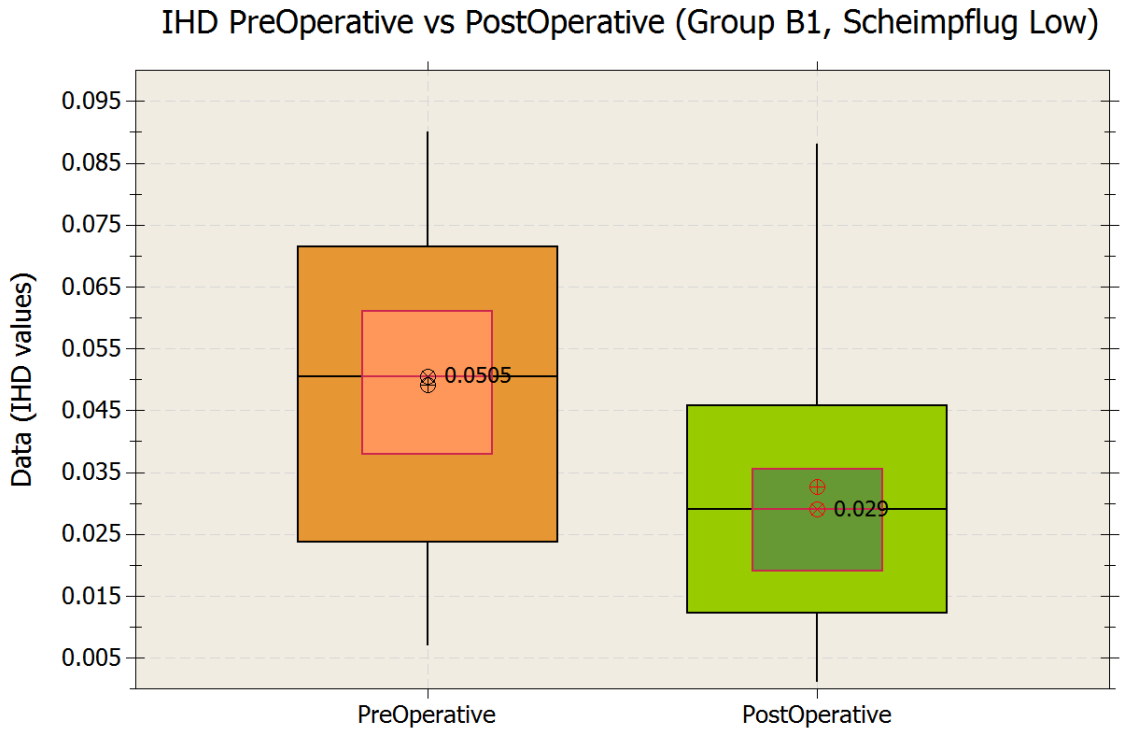

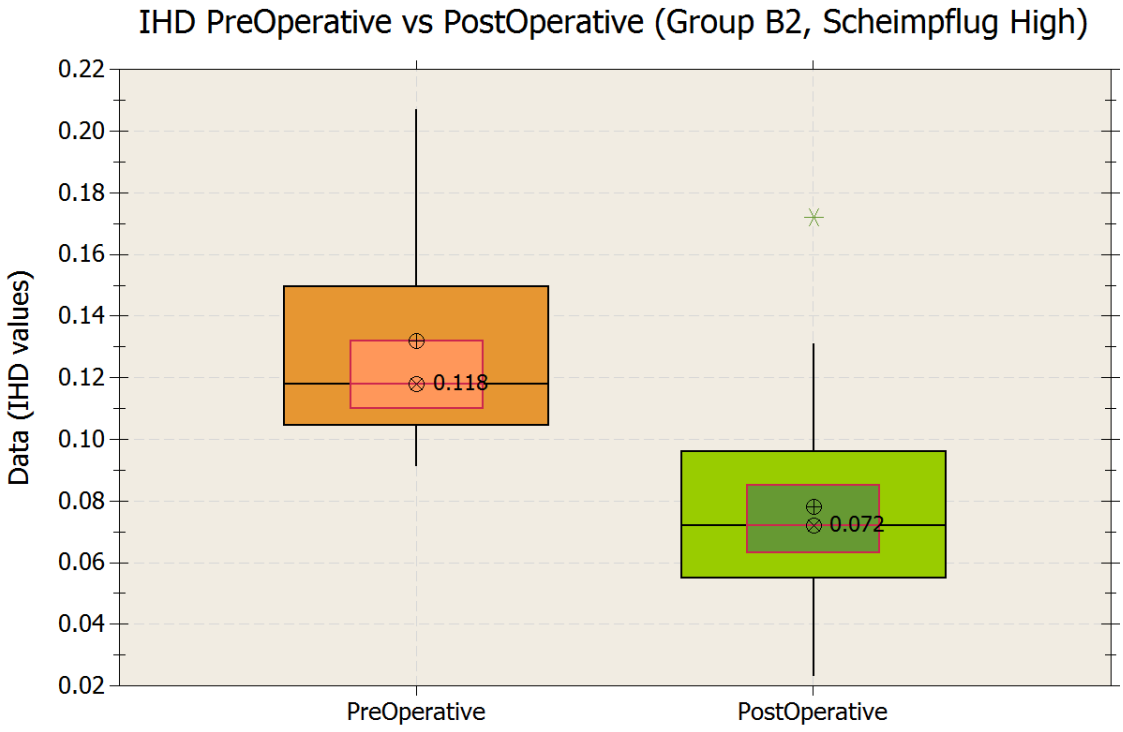

References

1. Krachmer JH, Feder RS, Belin MW. Keratoconus and related noninflammatory corneal thinning disorders. *Surv Ophthalmol.* 1984;28(4):293-322.

2. Belin MW, Asota IM, Ambrosio R Jr, Khachikian SS. What's in a name: keratoconus, pellucid marginal degeneration, and related thinning disorders. *Am J Ophthalmol.* 2011;152(2):157-162

3. Ambrósio R, Caldas DL, da Silva RS, Pimentel LN, de Freitas VB. Impact of the wavefront analysis in refraction of keratoconus patients. 2010 *Rev. Bras. Oftalmol.* 2010; 69 (5): 294-300

4. Kosaki R, Maeda N, Bessho K, Hori Y, Nishida K, Suzaki A, Hirohara Y, Mihashi T, Fujikado T, Tano Y. Magnitude and orientation of Zernike terms in patients with keratoconus. *Invest Ophthalmol Vis Sci.* 2007;48(7):3062-8.

5. Zadnik K, Steger-May K, Fink BA, Joslin CE, Nichols JJ, Rosenstiel CE, Tyler JA, Yu JA, Raasch TW, Schechtman KB; CLEK Study Group. Collaborative Longitudinal Evaluation of Keratoconus. Between-eye asymmetry in keratoconus. *Cornea.* 2002;21(7):671-9.

6. Jones-Jordan LA, Walline JJ, Sinnott LT, Kymes SM, Zadnik K. Asymmetry in keratoconus and vision-related quality of life. *Cornea.* 2013;32(3):267-72.

7. Chan E, Snibson GR. Current status of corneal collagen cross-linking for keratoconus: a review. *Clin Exp Optom*. 2013. doi: 10.1111/cxo.12020. [Epub ahead of print]

8. Lanchares E, del Buey MA, Cristóbal JA, Lavilla L, Calvo B. Biomechanical property analysis after corneal collagen cross-linking in relation to ultraviolet A irradiation time. *Graefes Arch Clin Exp Ophthalmol*. 2011;249(8):1223-7

9. Hafezi F, Kanellopoulos J, Wiltfang R, Seiler T. Corneal collagen crosslinking with riboflavin and ultraviolet A to treat induced keratectasia after laser in situ keratomileusis. *J Cataract Refract Surg. 2007* 33(12):2035-40.

10. Kanellopoulos AJ, Pe LH, Perry HD, Donnenfeld ED. Modified intracorneal ring segment implantations (INTACS) for the management of moderate to advanced keratoconus: efficacy and complications. *Cornea.* 2006;25(1):29-33.

11. Kanellopoulos AJ. Collagen cross-linking in early keratoconus with riboflavin in a femtosecond laser-created pocket: initial clinical results. *J Refract Surg.* 2009;25(11):1034-7.

12. Kanellopoulos AJ, Binder PS. Collagen cross-linking (CCL) with sequential topography-guided PRK: a temporizing alternative for keratoconus to penetrating keratoplasty. *Cornea.* 2007;26(7):891-5

13. Kanellopoulos AJ. Comparison of sequential vs same-day simultaneous collagen cross-linking and topography-guided PRK for treatment of keratoconus. *J Refract Surg.* 2009;25(9):S812-8.

14. Krueger RR, Kanellopoulos AJ. Stability of simultaneous topography-guided photorefractive keratectomy and riboflavin/UVA cross-linking for progressive keratoconus: case reports. *J Refract Surg.* 2010;26(10):S827-32

15. Kanellopoulos AJ, Asimellis G. Introduction of quantitative and qualitative cornea optical coherence tomography findings, induced by collagen cross-linking for keratoconus; a novel effect measurement benchmark. *Clin Ophthalmol.* 2013;7:329-35.

16. Kanellopoulos AJ. Managing Highly distorted corneas. Invited speaker lecture at the Subspecialty Day-Refractive Surgery, of the American Academy Of Ophthalmology, November 9th, 2007, 9.23-9.28am, New Orleans, USA.

17. Kanellopoulos AJ. Limited topography-guided surface ablation followed by stabilization with collagen cross-linking with UV irradiation and riboflavin for keratoconus, paper presentation, November 12th, 2007, 9.18-9.26am, New Orleans, USA.

18. Kanellopoulos AJ. Topography-Guided PRK combined with Cross-Linking for keratoconus and Post-LASIK Ectasia. Invited speaker at the International Refractive Surgery Symposia- Co-organized by ISRS, November 24th, 2007, 15.15-15.30pm, Istanbul, Turkey.

19. Perry H, Kanellopoulos AJ. Long term comparison of sequential to combined collagen cross linking and limited topography-guided PRK for keratoconus. Paper Presentation, International Congress of Corneal Cross Linking, Dec. 6th 2008, Session 3:11.45am-12.45pm, Dresden, Germany

20. Pantelis S., Kanellopoulos AJ. Novel keratoconus management with combined: topography-guided PR K(tPRK), femtosecond laser-assisted lamellar graft (fLK) and collagen cross linking (CCL). Paper Presentation, International Congress of Corneal Cross Linking, Dec. 6th 2008, Session 3:11.45am-12.45pm, Dresden, Germany

21. Kanellopoulos AJ. Long term results of a prospective randomized bilateral eye comparison trial of higher fluence, shorter duration ultraviolet A radiation, and riboflavin collagen cross linking for progressive keratoconus. *Clin Ophthalmol*. 2012:6 97–101.

22. Kanellopoulos AJ. Cross-linking plus topography-guided PRK for post-LASIK ectasia management. Chapter 22 In: *Mastering Advanced Surface Ablation Techniques*, Editors: Ashok Garg, Publisher: Jaypee Brothers 2007 p.204-14

23. Kanellopoulos AJ, Binder PS. Management of corneal ectasia after LASIK with combined, same-day, topography-guided partial transepithelial PRK and collagen cross-linking: the Athens protocol. *J Refract Surg*. 2011;27(5):323-31

24. Kanellopoulos AJ. Topography-guided hyperopic and hyperopic astigmatism femtosecond laser-assisted LASIK: long-term experience with the 400 Hz eye-Q excimer platform. *Clin Ophthalmol.* 2012;6:895-901.

25. Kanellopoulos AJ, Asimellis G. Long term bladeless LASIK outcomes with the FS200 femtosecond and EX500 excimer laser workstation: the Refractive Suite. *Clin Ophthalmol.* 2013;7:261-9

26. Kanellopoulos AJ, Asimellis G. High myopia one-year refractive and keratometric stability in LASIK with high-frequency femtosecond and excimer lasers. *J Refract Surg. 2013* (accepted for publication).

27. Kanellopoulos AJ, Asimellis G. Correlation Between Central Corneal Thickness, Anterior Chamber Depth, and Corneal Keratometry as Measured by Oculyzer II and WaveLight OB820 in Preoperative Cataract Surgery Patients. *J Refract Surg.* 2012;28(12):895-900.

28. Swartz T, Marten L, Wang M. Measuring the cornea: the latest developments in corneal topography. *Curr Opin Ophthalmol.* 2007;18(9):325-333.

29. Krumeich JH, Daniel J, Knulle A. Live-epikeratophakia for keratoconus. *J Cataract Refract Surg* 1998;24:456-63.

30. Li X, Yang H, Rabinowitz YS. Keratoconus: classification scheme based on videokeratography and clinical signs. *J Cataract Refract Surg* 2009; 35:1597–1603

31. Greenstein SA, Fry KL, Hersh PS. Corneal topography indices after corneal collagen crosslinking for keratoconus and corneal ectasia: one-year results. *J Cataract Refract Surg.* 2011;37(7):1282-90

32. Sonmez B, Doan MP, Hamilton DR. Identification of scanning slit-beam topographic parameters important in distinguishing normal from keratoconic corneal morphologic features. *Am J Ophthalmol.* 2007;143(3):401-8.

33. Ho JD, Tsai CY, Tsai RJ, Kuo LL, Tsai IL, Liou SW. Validity of the keratometric index: evaluation by the Pentacam rotating Scheimpflug camera. *J Cataract Refract Surg.* 2008;34(1):137-145.

34. Faria-Correia F, Ramos IC, Lopes BT, Salomão MQ, Luz A, Correa RO, Belin MW, and Ambrósio R Jr. Topometric and tomographic indices for the diagnosis of keratoconus. *Int J of Kerat and Ectatic Dis* 2012;1(2):100-06.

35. Rüfer F, Schröder A, Arvani MK, Erb C. Central and peripheral corneal pachymetry-standard evaluation with the Pentacam system [German]. *Klin Monbl Augenheilkd*. 2005;222(2):117-122.

36. Emre S, Doganay S, Yologlu S. Evaluation of anterior segment parameters in keratoconic eyes measured with the Pentacam system. *J Cataract Refract Surg.* 2007;33(10):1708-1712.

37. Kanellopoulos AJ, Asimellis G. Revisiting Keratoconus classification based on the evaluation corneal asymmetry indices, derived from Scheimpflug imaging. *Clin Ophthalmol*. 2013 (accepted for publication).

38. Gordon-Shaag A, Millodot M, Shneor E. The Epidemiology and Etiology of Keratoconus. *Int J Keratoco Ectatic Corneal Dis.* 2012;1(1):7-15.

39. Markakis GA, Roberts CJ, Harris JW, Lembach RG. Comparison of Topographic Technologies in Anterior Surface Mapping of Keratoconus using Two Display Algorithms and Six Corneal Topography Devices. *Int J of Kerat and Ectatic Dis.* 2012;1(3):153-157

40. Koller T, Iseli HP, Hafezi F, Vinciguerra P, Seiler T. Scheimpflug imaging of corneas after collagen cross-linking. *Cornea.* 2009;28(5):510-5.

41. Scarcelli G, Kling S, Quijano E, Pineda R, Marcos S, Yun SH. Brillouin microscopy of collagen crosslinking: noncontact depth-dependent analysis of corneal elastic modulus. *Invest Ophthalmol Vis Sci.* 2013;54(2):1418-25.

42. Maeda N, Klyce SD, Smolek MK, Thompson HW. Automated keratoconus screening with corneal topography analysis. *Invest Ophthalmol Vis Sci* 1994;35:2749-57.

43. Dubbelman M, Weeber HA, van der Heijde RG, Völker-Dieben HJ. Radius and asphericity of the posterior corneal surface determined by corrected Scheimpflug photography. *Acta Ophthalmol Scand*. 2002;80(4):379-83.

44. Ambrósio R Jr, Caiado AL, Guerra FP, Louzada R, Roy AS, Luz A, Dupps WJ, Belin MW. Novel pachymetric parameters based on corneal tomography for diagnosing keratoconus. *J Refract Surg.* 2011;27(10):753-8.

45. Hersh PS, Greenstein SA, Fry KL. Corneal collagen crosslinking for keratoconus and corneal ectasia: one-year results. *J Cataract Refract Surg* 2011; 37:149–160

46. Mencucci R, Paladini I, Virgili G, Giacomelli G, Menchini U. Corneal thickness measurements using time-domain anterior segment OCT, ultrasound, and Scheimpflug tomographer pachymetry before and after corneal cross-linking for keratoconus. *J Refract Surg.* 2012;28(8):562-6.

47. Vinciguerra P, Albe E, Trazza S, Rosetta P, Vinciguerra R, Seiler T, Epstein D. Refractive, topographic, tomographic, and aberrometric analysis of keratoconic eyes undergoing corneal cross-linking. *Ophthalmology* 2009; 116:369–378

48. Raiskup-Wolf F, Hoyer A, Spoerl E, Pillunat LE. Collagen crosslinking with riboflavin and ultraviolet-A light in keratoconus: longterm results. *J Cataract Refract Surg* 2008; 34:796–801

ORIGINAL RESEARCH

Revisiting Keratoconus classification based on the evaluation corneal asymmetry indices, derived from Scheimpflug imaging.

Anastasios John Kanellopoulos, M.D. [1,2]

George Asimellis, Ph.D. [1]

[1] Laservision.gr Eye Institute, Athens, Greece

[2] New York University School of Medicine, NY, USA

Correspondence: Professor A. John Kanellopoulos, MD

17 Tsocha str. Athens, Greece Postal Code 11521

Tel +30 210 747 2777

Fax +30 210 747 2789

Email ajk@brilliantvision.com

Acknowledgments/Disclosures

None.

Abstract

Purpose

To survey the standard keratoconus grading scale (Pentacam-derived Amsler & Krumeich stages) compared to corneal regularity indices, measured by the Pentacam and to best spectacle corrected distance visual acuity.

Patients and methods

Two hundred twelve (212) keratoconic cases were evaluated for the keratoconic grading and anterior surface indexing by Pentacam imaging, as well as for subjective refraction, measured by the best-spectacle corrected distance visual acuity (CDVA). The correlations between CDVA, keratometry, and the Scheimpflug keratoconic grading and the seven anterior – surface Pentacam-derived topometric indices (Indices of; surface variance, vertical asymmetry, keratoconus index, central keratoconus index, height asymmetry, height decentration, minimum radius of curvature) were analyzed using paired two-tailed t-tests, coefficient of determination (r^2), and trend line linearity.

Results

Average CDVA (expressed decimally) was, for all eyes: (average ± standard deviation) 0.626 ± 0.244, range (max-min) 1.00 to 0.10). Average flat meridian keratometry was (K1) 46.7 ± 5.89 diopters (D), and for the steep, (K2), 51.05 ± 6.59 D.

The correlations between CDVA, keratometry, the seven Scheimpflug-derived topometric indices with the Pentacam-derived keratoconus severity grading were investigated. The index of height decentration (ISV), and the Index of height decentration (IHD), had the strongest correlate for keratoconus to the value of $P < 0.001$. CDVA and keratometry were correlated poorly.

Conclusions

We report herein for the first time that the ISV and IHD, may be the most sensitive and specific criteria in the diagnosis, progression, and surgical follow-up in keratoconus. The classification proposed herein, may present a novel benchmark in clinical work and future studies.

Keywords

Keratoconus diagnosis and classification; Pentacam topometric indices; keratoconus topography diagnosis; Amsler & Krumeich keratoconus grading, index of surface variance, index of vertical asymmetry, keratoconus index, central keratoconus index, index of height asymmetry, index of height decentration, index of minimum radius of curvature.

Introduction

Keratoconus (KCN) is described as a degenerative bilateral, progressive, noninflammatory disorder characterized by ectasia, thinning, and increased curvature. [1,2] It is associated with loss of visual acuity particularly in relation to progressive cornea irregularity [3,4] and usually is manifested asymmetrically between the two eyes of the same patient. [5,6]

Occasionally, the patient may present with symptoms of photophobia, glare and monocular diplopia.

The problem of specificity and sensitivity of keratoconus assessment, particularly the diagnosis of early signs of ectasia and/or subclinical keratoconus, and for monitoring the progression of the disease, has been extensively studied. [7] The common used options for the clinician usually include optically-based anterior segment imaging modalities, such as Placido corneal topography [8,9] and slit or Scheimpflug imaging [10] that provide curvature qualitative and quantitative data.

Anterior Segment Topometric Indices

Rotating camera Scheimpflug imagery provides a multitude of corneal topometry measurements. [11] Data include refractive (keratometric), tomographic, and pachymetric mapping. [12] In addition, specific anterior-surface curvature regularity indices have been developed for the grading and classification of keratoconus stages, as well as the post-operative assessment [13-19] which can be provided by the Pentacam software (Oculus Optikgeräte GmbH, Wetzlar, Germany).

This study aims to investigate these values, the repeatability of their measurement, the correlation of the above indices with CDVA, keratometry as well as with commonly used keratoconus classification, in a large pool of clinically-diagnosed keratoconic eyes.

Materials and methods

This study received approval by the Ethics Committee of our Institution, adherent to the tenets of the Declaration of Helsinki. Informed consent was obtained from each subject at the time of the first clinical visit. These cases were studied over the span of at least two years.

Patient inclusion criteria

The study group consisted of two hundred twelve (212) cases presented to our institution. Subjects' ages ranged from 19–57 (average 31.9 ± 7.5 years).

Each case was subjected to a complete ocular examination, including subjective refraction, CDVA measurement with this refraction, and slit-lamp biomicroscopy for clinical signs of keratoconus.

Inclusion criteria included a minimum age of 18 years and definite findings consistent with keratoconus, such as described by the Collaborative Longitudinal Evaluation of Keratoconus (CLEK) group. [20] Exclusion criteria included systemic disease, previous corneal surgery, history of chemical injury or delayed epithelial healing, and pregnancy or lactation during the study (for the female patients).

Imaging, measurement and analysis

Anterior segment measurements on all subjects including anterior segment imaging measurements with the Pentacam Scheimpflug rotating camera. The device was calibrated according to manufacturer recommendations prior to undertaking the measurements. The Pentacam measurements were obtained and processed via the Examination Software (Version 1.17r47).

For each eye, four consecutive measurements were obtained and processed to test for data acquisition repeatability. The default settings of twenty-five images per single acquisition was used.

Linear regression analysis was performed to seek possible correlations. Descriptive and comparative statistics, analysis of variance between keratoconus Amsler & Krumeich stage subgroups and linear regression were performed with statistics tools provided by Minitab version 1.6.1 (MiniTab Ltd., Coventry, UK) and Origin Lab version 9 (OriginLab Corp, Northampton, MA). Paired analysis p-values less than 0.05 were considered indication of statistically significant results.

Results

Keratometric and anterior-segment topographic indices statistics

The sample population consisted of 212 cases of which 65 were female patients and 147 male patients. There is a preponderance towards male population, consistent with our clinical experience in male-female incidence in keratoconic patients, [21] and keratoconus incidence studies. [22] Of the 212 eyes, 113 were right (OD) and 99 were left (OS). Average age was, for all patients, 31.77 ± 7.23 (57-19) years of age.

Average CDVA (expressed decimally) was, for all eyes: (average ± standard deviation) 0.626 ± 0.244, range (max-min) 1.00 to 0.10. Average, standard deviation, maximum and minimum corneal surface keratometry, and topometric indices for all eyes in the study are reported in Table 1. Intraindivicual repeatability was assessed via the standard deviation of the four consecutive measurements undertaken per each eye. Average and standard deviation of repeatability for the seven topometric indices in all 212 eyes measured is reported in Table 2.

The sample was presented with an average keratometry on the anterior surface flat axis of 46.7 ± 5.89 keratometric diopters (D), and for the steep axis of 51.05 ± 6.59 D. Our statistical analysis showed that 95% of the sample population had a steep axis keratometry > 46.025 D, consistent with the CLEK group standards. [20]

Topographic indices correlation with CDVA

Paired statistics between CDVA and the IHD, ISV, IVA, KI, CKI, IHA, and Rmin indices (in 8 mm zone), and specifically, coefficient of determination (r^2) and Pearson linear regression data between CDVA and the IHD, ISV, IVA, KI, CKI, IHA and Rmin indices within all eyes in the study group (n = 212) are reported in Table 3.

The correlations between the seven keratoconic anterior – surface topometric indices with CDVA are illustrated in Figures 3a-g. Specifically, the scatter and fitted line plots of ISV (3a), IVA (3b), KI (3c), CKI (3d), IHA (3e), ISD (3f), and Rmin (3g) vs CDVA are plotted, in addition with the 95% confidence (CI) and 95% prediction interval (PI) lines. The paired data present with coefficient of determination (r^2) of linear correlation with CDVA of: ISV, 0.55; IVA, 0.34; KI, 0.424; CKI, 0.396; IHA, 0.107; IHD, 0.393, and Rmin, 0.516. Respectively, the Pearson correlation values vs CDVA were for ISV, -0.746; IVA, -0.584; KI, -0.680; CKI, -0.642; IHA, -0.344, ISD, -0.627, and Rmin, 0.718. In all cases, p-value was < 0.0001. (Table 3).

Topographic indices correlation with Keratoconus stages grading

The 212 eyes were subjected to keratoconus Amsler & Krumeich stages grading [23] by the Pentacam software. The resulting grading designated n1 = 10 eyes as KC1, n12 = 11 eyes as KC12, n2 = 32 eyes as KC2, n23= 22 eyes as KC2-3, n3 = 54 eyes as KC3, n34 = 45 eyes as KC34, and n4 = 4 eyes as KC4.

The correlations between CDVA, the seven Scheimpflug anterior – surface keratometric and topometric indices with the above keratoconus grading are illustrated in Figures 2a-h, showing box plots with the median level and value (also indicated by the symbol ⊗), the

average point (indicated by the symbol ⊕), the 95% median confidence range box (black line boxes), and the interquartile intervals range box (red line boxes). Descriptive statistics for the keratoconus grading subgroups for CDVA and the seven topometric indices are presented in Table 4, and two-sample T-test results (not assuming equal variances) between the keratoconus grading subgroups for CDVA and the seven topometric indices are presented in Table 5.

Discussion

The Pentacam software compares the measured values with the means and standard deviations of a normal population, and, helps provide color-coded 'flags'. For example, measured values which exceed the standard deviation by a factor of more than 2.5 are classified as abnormal and highlighted in yellow, and pathological values, i.e. values that exceed the standard deviation by a factor of more than 3, are highlighted in red.

Namely, these indices are the following:

(a) the Index of Surface Variance (ISV), the value of deviation of individual corneal radii from the mean curvature. ISV is thus an expression of the corneal surface irregularity. It is elevated in all types of corneal surface irregularity (scars, astigmatism, deformities caused by contact lenses, pachymetric, etc). According to the manufacturer's user manual, [24] an ISV larger than 37 is considered abnormal (marked with yellow), and larger than 41, pathological (red).

(b) the Index of Vertical Asymmetry (IVA), which is a measure of the difference between superior and inferior corneal curvature (similar to the commonly used I–S ratio). [25] IVA is thus the value of curvature symmetry, with respect to the horizontal meridian as axis of reflection. An IVA larger than 0.28 is considered abnormal, and larger than 0.32, pathological.

(c) The Keratoconus Index (KI). KI increases with severity of keratoconus, and is sometimes referred to as pachymetric index. KI value larger than 1.07 is considered abnormal and/or pathological.

(d) The Central Keratoconus Index (CKI). CKI is elevated especially in central pachymetric, and increases with the severity of central keratoconus. CKI value larger than 1.03 is considered abnormal and/or pathological.

(e) The Index of Height Asymmetry (IHA), calculated by the height data symmetry comparison of the superior and inferior area, and provides the degree of symmetry of height data with respect to the horizontal meridian as axis of reflection. IHA is a similar to the IVA, but based on corneal elevation, and thus it is more sensitive. An IHA value larger than 19 is considered abnormal, and larger than 21, pathological.

(f) the Index of Height Decentration (IHD). IHD is the value of the decentration of elevation data in the vertical direction, and is calculated from a Fourier analysis. This index provides the degree of decentration in the vertical direction. An IHD value larger than 0.014 is considered abnormal, and larger than 0.016, pathological.

(g) The minimum radius of curvature (Rmin), expressed in mm. Rmin is a measurement of the smallest radius of sagittal corneal curvature (ie, the maximum steepness of the cone). Values of Rmin less than 6.71 mm are considered abnormal and/or pathological, considering that the average radius of the anterior corneal surface is 7.87 ± 0.27 mm. [26]

Association with these indices with clinical keratoconus observations is provided by the manufacturer and are listed in Table 6.

The clinical suspicion of early-stage keratoconus may be based on refraction criteria such as a change in refractive power and the axis of astigmatism, fluctuating refraction and several clinical findings (such as conspicuous retinoscopy sings). Optical imaging, such as topometry and topography, provides valuable supplementary information, and has been long supported that the contribution of proper evaluation and analysis of anterior surface

irregularity derived from topography, [27] or more recently, from Pentacam topometry, like the seven topographic indices studied in this manuscript, may provide an invaluable aid in the diagnosis and progression evaluation of the disease. [28] We only identified two reports published in this matter of correlation of the above Pentacam-derived indices, and specifically with best spectacle corrected distance visual acuity (CDVA) [29] and the severity of keratoconus classification. [30]

The correlation (Table 3, and figures 3) between the seven anterior-segment topographic indices and CDVA is not very strong. The Rmin ($r^2 = 0.516$, $P < 0.001$) and ISV ($r^2 = 0.557$, $P < 0.001$) were found to be the strongest-correlated indices with CDVA compared to the other indices. The least correlated index was IHA ($r^2 = 0.107$, $P < 0.001$). This could be a result of significantly worse intraindividual repeatability of this index, possibly as a result of the complicated nature of its algorithm. As indicated in Table 2, repeatability, measured by the standard deviation of the measured index over four consecutive acquisitions, was as low as 1.50%, on average, for Rmin, and up to 4.6% for IHD and IVA; however, the IHA index had a distinctively 43.78% average standard deviation among any four consecutive measurements. In addition, the IHA index had the worst-correlation with keratoconus severity (Figure 2f), with two stages not statistically significantly distinguished, and the remaining also border-line.

Our study is indicating that the correlation between keratoconus severity and the anterior-segment topographic indices can be better described with the ISV (with the exception of the highest stage KC4, all other P-values were < 0.001, as seen in Table 5), followed by the IHD (with the exception of the lowest stage KC1, all other P-values were < 0.001).

Our results indicate that the visual performance in keratoconus was nor clearly predicable for keratoconus severity, and thus CDVA cannot be a dependable indicator of keratoconus severity and/or progression, and thus cannot be employed in the postoperative assessment

of operations aiming to arrest the keratoconus progression such as cross-linking with riboflavin (CXL). [31] It is customary to assess severity based on visual function and as noted above this can be deceiving. Clinicians must be cautious. For example, the data presented in this work (Figure 2a) suggest that CDVA is not very well correlated with the keratoconus severity, as the spread of CDVA measurements within the same 'severity stage', eg. KC3, KC3-4 was found to be too large. The average coefficient of determination (r^2) was in the order of 0.5, in agreement with previous studies[32]

The above results are in agreement with our past clinical experience with significant number of keratoconic patients followed for over 15 years. Our observation has been that visual acuity can present with large variations, and sometimes unexpectedly good for the corresponding keratometry and overall corneal asymmetry. This may be due to a 'multifocal' and 'soft', ie adaptable cornea, in addition to possible advanced neural processing development in the individual. These 'advantages', however, are to a large degree compromised with a CXL procedure applied in young (18 to 25 years old) keratoconus patients in our long term clinical observations.

Although not specifically studied herein, our clinical assessment of this group is that CDVA is poorly correlated to keratoconus severity mainly in younger patients. As older keratoconus patients were encountered (over 30 years old and in most over 40), their CDVA started to correlate to the ISV and IHD. This observation poses an even greater reason for clinicians to employ the strongest clinical suspicion in younger patients that may be at risk for developing keratoconus and maybe labeled "normal" if a very good CDVA performance is achieved by them.

This maybe explained by the higher elasticity, of the pathologic cornea in younger keratoconus patients. This age-related difference may allow them to accomplish high CDVA

values with monocular testing by squinting and/or head tilting. ISV and IHD assessment in the younger patients with relative low keratometric values may be the crucial factor in early diagnosis of keratoconus.

Conclusions

The index of surface variance (ISV) and the index of height decentration (IHA), both derived from Scheimpflug corneal imaging, may be more sensitive and specific tools than corrected visual acuity, in evaluating early diagnosis, and possible progression in keratoconus patients and corneal ectasia. They may become a novel benchmark for future studies, and may aid in the development of new keratoconus diagnostic and follow-up criteria.

Tables

Table 1

Collective average, standard deviation (StDev), maximum (Max) and minimum (Min) anterior keratometry, and topometric indices, as measured in the 8 mm zone. Abbreviations: ISV, Index of Surface Variance; IVA, Index of Vertical Asymmetry; KI, Keratoconus Index; CKI, Central Keratoconus Index; IHA, Index of Height Asymmetry; IHD, Index of Height Decentration; Rmin, Smallest sagittal curvature; CDVA, best- spectacle corrected distance visual acuity.

		Average	StDev	Max	Min
Anterior Cornea	K1 – flat (D)	46.78	± 5.89	78.50	33.70
	K2 – steep (D)	51.05	± 6.59	80.70	42.10
	Km – mean (D)	48.80	± 6.05	78.80	40.60
	Astigmatism (D)	-2.10	± 6.05	+11.30	-12.40
Anterior surface topometric indices	ISV	98.99	± 47.43	262	14
	IVA	1.05	± 0.52	2.52	0.09
	KI	1.28	± 0.17	1.83	0.97
	CKI	1.06	± 0.07	1.30	0.90
	IHA	30.60	± 22.21	103.00	0.20
	IHD	0.091	± 0.054	0.256	0.005
	Rmin (mm)	6.07	± 0.88	7.73	3.30
CDVA	decimal	0.63	± 0.25	1.00	0.10

Table 2

Intraindividual repeatability measurements for the seven anterior surface topometric indices, resulting as the standard deviation (%) of the four consecutive acquisitions on each eye.

Abbreviations: ISV, Index of Surface Variance; IVA, Index of Vertical Asymmetry; KI, Keratoconus Index; CKI, Central Keratoconus Index; IHA, Index of Height Asymmetry; IHD, Index of Height Decentration; CDVA, best- spectacle corrected distance visual acuity.

	ISV	IVA	KI	CKI	IHA	IHD	Rmin
average	2.77%	4.63%	2.15%	2.02%	43.78%	4.67%	1.50%
Stdev (±)	1.32%	1.94%	1.27%	0.66%	7.18%	1.62%	0.68%

Table 3

Coefficient of determination (r^2) and Pearson correlation data between CDVA and the IHD, ISV, IVA, KI, CKI, IHA and Rmin indices within all eyes in the study group (n =212). Abbreviations: ISV, Index of Surface Variance; IVA, Index of Vertical Asymmetry; KI, Keratoconus Index; CKI, Central Keratoconus Index; IHA, Index of Height Asymmetry; IHD, Index of Height Decentration; CDVA, best- spectacle corrected distance visual acuity. In all cases, $p < 0.001$.

		CDVA	IHD	ISV	IVA	KI	CKI	IHA
Pearson correlation	IHD	-0.627						
(r^2)		0.393						
Pearson correlation	ISV	-0.746	0.91					
(r^2)		0.55						
Pearson correlation	IVA	-0.584	0.893	0.878				
(r^2)		0.340						
Pearson correlation	KI	-0.680	0.891	0.911	0.845			
(r^2)		0.424						
Pearson correlation	CKI	-0.642	0.616	0.721	0.436	0.73		
(r^2)		0.396						
Pearson correlation	IHA	-0.344	0.524	0.484	0.422	0.467	0.252	
(r^2)		0.107						
Pearson correlation	Rmin	0.718	-0.799	-0.864	-0.623	-0.790	-0.787	-0.541
(r^2)		0.516						

Table 4: Descriptive Statistics for the keratoconus grading subgroups for Age, CDVA and the seven topometric indices. Abbreviations: Stdev: standard deviation; SE mean, standard error of the mean

Keratoconus Grading	KC1	KC-12	KC2	KC-23	KC3	KC-34	KC4
Age (years)							
Mean	31.0	32.5	31.3	31.3	30.9	30.6	31.0
StDev (±)	8.4	7.6	7.8	6.0	6.7	7.3	8.4
CDVA							
Mean	0.907	0.779	0.695	0.64	0.55	0.416	0.2225
StDev (±)	0.107	0.166	0.202	0.133	0.188	0.187	0.0634
SE Mean	0.034	0.05	0.036	0.028	0.026	0.028	0.032
ISV							
Mean	40.6	50.91	72.75	93.77	114.07	157.8	218.8
StDev (±)	2.88	3.56	9.32	5.25	9.51	17.9	29
SE Mean	0.91	1.1	1.6	1.1	1.3	2.7	14
IVA							
Mean	0.422	0.5618	0.855	1.068	1.219	1.612	2.002
StDev (±)	0.0735	0.0994	0.134	0.194	0.258	0.361	0.497
SE Mean	0.023	0.03	0.024	0.041	0.035	0.054	0.25
KI							
Mean	1.10	1.12	1.1838	1.2664	1.3291	1.47	1.7475
StDev (±)	0.0163	0.0335	0.0522	0.027	0.0547	0.121	0.0929
SE Mean	0.0052	0.01	0.0092	0.0058	0.0075	0.018	0.046

CKI							
Mean	1.014	1.0145	1.0291	1.05	1.0711	1.1269	1.208
StDev (±)	0.0135	0.023	0.0352	0.0385	0.0394	0.0702	0.101
SE Mean	0.0043	0.0069	0.0062	0.0082	0.0054	0.01	0.051

IHA							
Mean	18.05	20.55	26.5	33.3	37.7	39.3	61.7
StDev (±)	9.66	7.68	15.6	17.3	19.3	28.8	14.4
SE Mean	3.1	2.3	2.7	3.7	2.6	4.3	7.2

IHD							
Mean	0.031	0.04355	0.0677	0.0878	0.1063	0.1512	0.24
StDev (±)	0.00723	0.00972	0.0183	0.0169	0.0266	0.0373	0.0185
SE Mean	0.0023	0.0029	0.0032	0.0036	0.0036	0.0056	0.0093

Rmin (mm)							
Mean	6.922	6.755	6.52	6.104	5.775	5.146	4.165
StDev (±)	0.311	0.275	0.463	0.483	0.381	0.675	0.513
SE Mean	0.098	0.083	0.082	0.1	0.052	0.1	0.26

Table 5: Two-Sample T-test results, not assuming equal variances, between successive pairs of keratoconus severity stages subgroups for CDVA and the seven topometric indices. CI: Confidence interval.

CDVA	K1 vs K1-2	K12 vs K2	K2 vs K2-3	K2-3 vs K3	K3 vs K3-4	K3-4 vs P4
Estimate for difference:	-0.1279	-0.0838	-0.0558	-0.0892	-0.1344	-0.1935
95% CI for difference:	(-0.2552, -0.0006)	(-0.2115, 0.0440)	(-0.1473, 0.0357)	(-0.1657, -0.0127)	(-0.2095, -0.0593)	(-0.2890, -0.0980)
T-Value	-2.12	-1.36	-1.22	-2.34	-3.55	-4.58
P-Value	0.049	0.187	0.227	0.023	0.001	0.001

ISV	K1 vs K1-2	K12 vs K2	K2 vs K2-3	K2-3 vs K3	K3 vs K3-4	K3-4 vs P4
Estimate for difference:	10.31	21.84	21.02	20.3	43.7	61
95% CI for difference:	(7.35, 13.27)	(17.87, 25.82)	(17.02, 25.03)	(16.88, 23.72)	(37.79, 49.62)	(14.1, 107.8)
T-Value	7.33	11.1	10.55	11.86	14.76	4.14
P-Value	<0.001	<0.001	<0.001	<0.001	<0.001	0.026

IVA	K1 vs K1-2	K12 vs K2	K2 vs K2-3	K2-3 vs K3	K3 vs K3-4	K3-4 vs P4
Estimate for difference:	0.1398	0.2929	0.2135	0.1503	0.3939	0.39
95% CI for difference:	(0.0602, 0.2195)	(0.2139, 0.3718)	(0.1167, 0.3103)	(0.0414, 0.2592)	(0.2660, 0.5218)	(-0.419, 1.199)

T-Value	3.69	7.67	4.48	2.77	6.13	1.53
P-Value	0.002	<0.001	<0.001	0.008	<0.001	0.222

KI	K1 vs K1-2	K12 vs K2	K2 vs K2-3	K2-3 vs K3	K3 vs K3-4	K3-4 vs P4
Estimate for difference:	0.02	0.0638	0.0826	0.06271	0.1414	0.2771
95% CI for difference:	(-0.0043, 0.0443)	(0.0357, 0.0918)	(0.0607, 0.1045)	(0.04394, 0.08148)	(0.1024, 0.1804)	0.1186, 0.4356)
T-Value	1.76	4.66	7.59	6.66	7.26	5.56
P-Value	0.099	<0.001	<0.001	<0.001	<0.001	0.011

CKI	K1 vs K1-2	K12 vs K2	K2 vs K2-3	K2-3 vs K3	K3 vs K3-4	K3-4 vs P4
Estimate for difference:	0.00055	0.01452	0.0209	0.02111	0.0558	0.0806
95% CI for difference:	(-0.01670, 0.01779)	(-0.00459, 0.03362)	(0.0001, 0.0417)	(0.00126, 0.04096)	(0.0323, 0.0792)	(-0.0842, 0.2454)
T-Value	0.07	1.56	2.03	2.15	4.75	1.56
P-Value	0.947	0.131	0.049	0.038	<0.001	0.217

IHA	K1 vs K1-2	K12 vs K2	K2 vs K2-3	K2-3 vs K3	K3 vs K3-4	K3-4 vs P4
Estimate for difference:	2.5	5.93	6.82	4.38	1.58	22.44
95% CI for difference:	(-5.58, 10.59)	(-1.37, 13.22)	(-2.45, 16.10)	(-4.74, 13.50)	(-8.45, 11.60)	(0.90, 43.98)

T-Value	0.65	1.65	1.48	0.97	0.31	2.68
P-Value	0.522	0.108	0.145	0.338	0.755	0.044

IHD	K1 vs K1-2	K12 vs K2	K2 vs K2-3	K2-3 vs K3	K3 vs K3-4	K3-4 vs P4
Estimate for difference:	0.01255	0.02411	0.02012	0.01856	0.04487	0.0888
95% CI for difference:	(0.00474, 0.02035)	(0.01522, 0.03300)	(0.01038, 0.02985)	(0.00836, 0.02876)	(0.03165, 0.05808)	(0.0610, 0.1166)
T-Value	3.38	5.52	4.16	3.64	6.76	8.21
P-Value	0.003	<0.001	<0.001	0.001	<0.001	<0.001

Rmin (mm)	K1 vs K1-2	K12 vs K2	K2 vs K2-3	K2-3 vs K3	K3 vs K3-4	K3-4 vs P4
Estimate for difference:	-0.167	-0.235	-0.416	-0.329	-0.629	-0.981
95% CI for difference:	(-0.438, 0.103)	(-0.473, 0.003)	(-0.681, -0.151)	(-0.563, -0.094)	(-0.855, -0.403)	(-1.858, -0.104)
T-Value	-1.30	-2.02	-3.16	-2.85	-5.56	-3.56
P-Value	0.209	0.053	0.003	0.008	<0.001	0.038

Table 6

Classification stages of keratoconus adapted from the classical Amsler & Krumeich standards. [30] Best spectacle corrected distance visual acuity (CDVA) correction, with topography-based graduation indices (ISV, Index of Surface Variance; KI, Keratometry Index) compared with retinoscopy signs and clinical corneal slit lamp observations. Adapted from Oculyzer User Manual. [24]

	CDVA	ISV	KI	Other indices	Rmin	Retinoscopy signs	Cornea Slit Lamp Observations
Pre-stage (early signs)	20/20 to 20/15	< 30	1.04 to 1.07	all 4 indices are 'normal'	7.8 to 6.7 mm	No clear light or shadow movement.Hint of 'scissors' effect	Clear cornea, unobtrusive. Horizontal, oval, or round shades central or slightly decentered, when observed under direct ophthalmoscopy.
Level 1	20/25 to 20/15	30 to 55	1.07 to 1.15	sometimes one value within the 'abnormal' range	7.5 to 6.5 mm	Distorted retinoscopic reflex. Scissors effect.	Clear cornea. Fleischer's ring at the apex base. Cone and cone base clearly visible with direct ophthalmoscopy. Decrease in apex thickness not visible, but measureable.
Level 2	20/60 to 20/20	55 to 90	1.10 to 1.25	often one value within the 'abnormal' range	6.9 to 5.3 mm	Clear scissors effect, retinoscopy difficult to perform.	Often cornea still clear, apex slightly thinner and eventually decentered. Partial or circular Fleischer' ring. Voght strieae may be visible.

Level 3	20/125 to 20/30	90 to 150	1.15 to 1.45	at least one value within the 'abnormal' range	6.6 to 4.8 mm	Distinct scissors effect, retinoscopy nearly impossible to perform.	Apex thinner, decentered, and often slightly cloudy. Clear and mostly circular Fleischer' ring. Voght strieae clearly visible. Eventually Munson-sign may appear.
Level 4	<20/400 to 20/100	> 150	> 1.50	at least one value within the 'abnormal' range	< 5.00 mm	Retinoscopy impossible to perform.	Cornea often scarred and opaque in the apex. Munson-sign evident.

Figures

Figure 1

Scatter and Fitted Line Plot of the seven anterior-surface parameters vs CDVA (best- spectacle corrected distance visual acuity) with 95% confidence intervals (CI) and 95% prediction intervals (PI).

1a ISV (Index of Surface Variance) vs CDVA

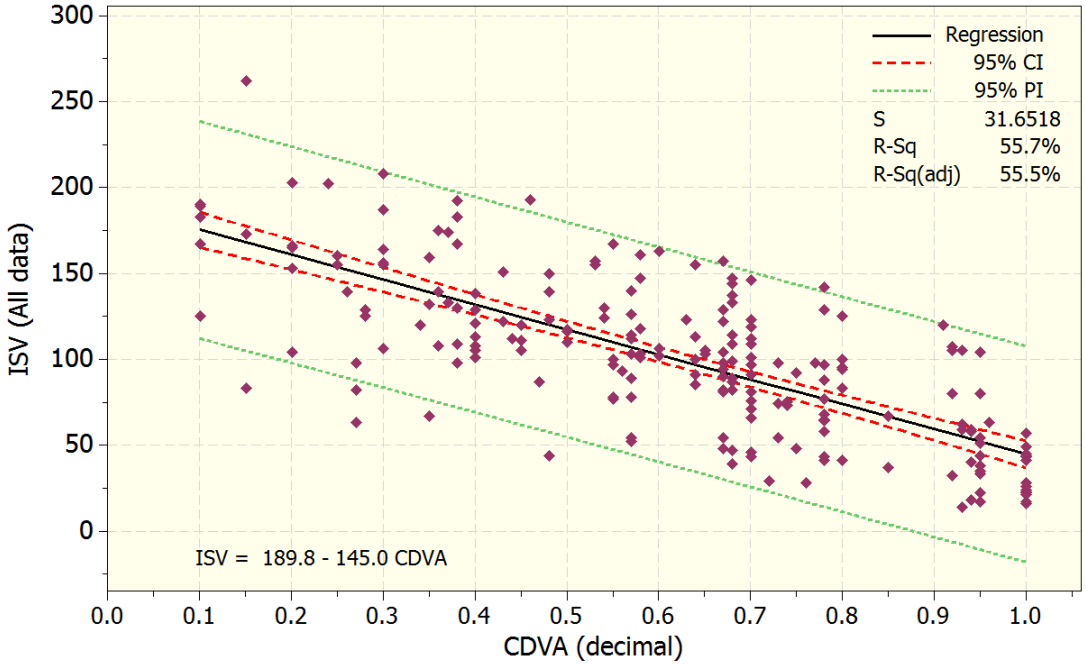

1b IVA (Index of Vertical Asymmetry) vs CDVA

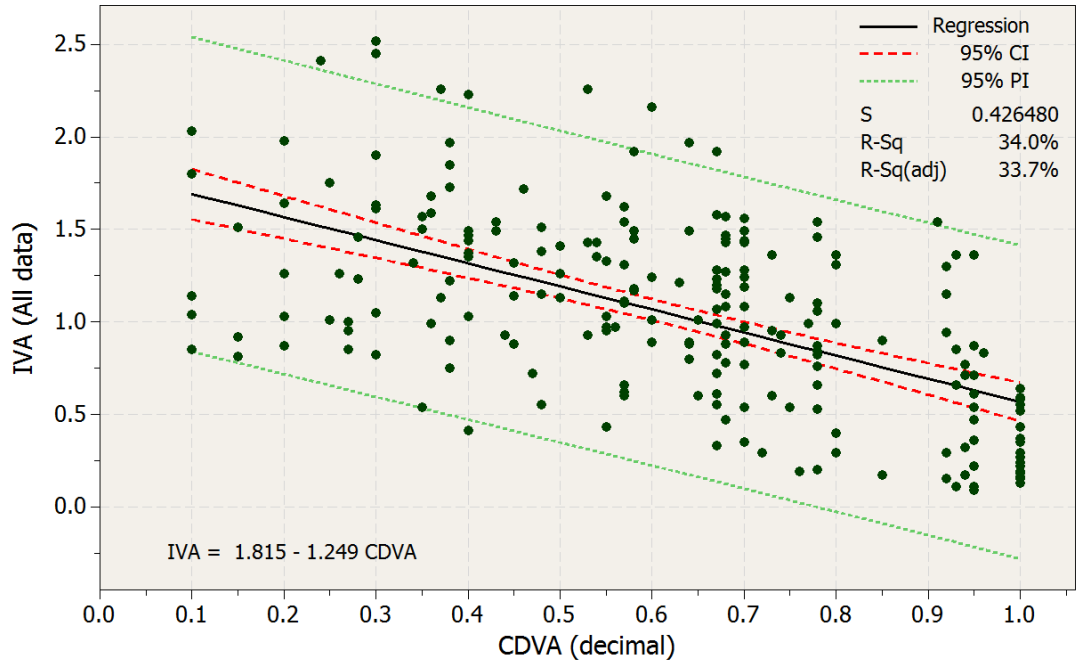

1c KI (Keratoconus Index) vs CDVA

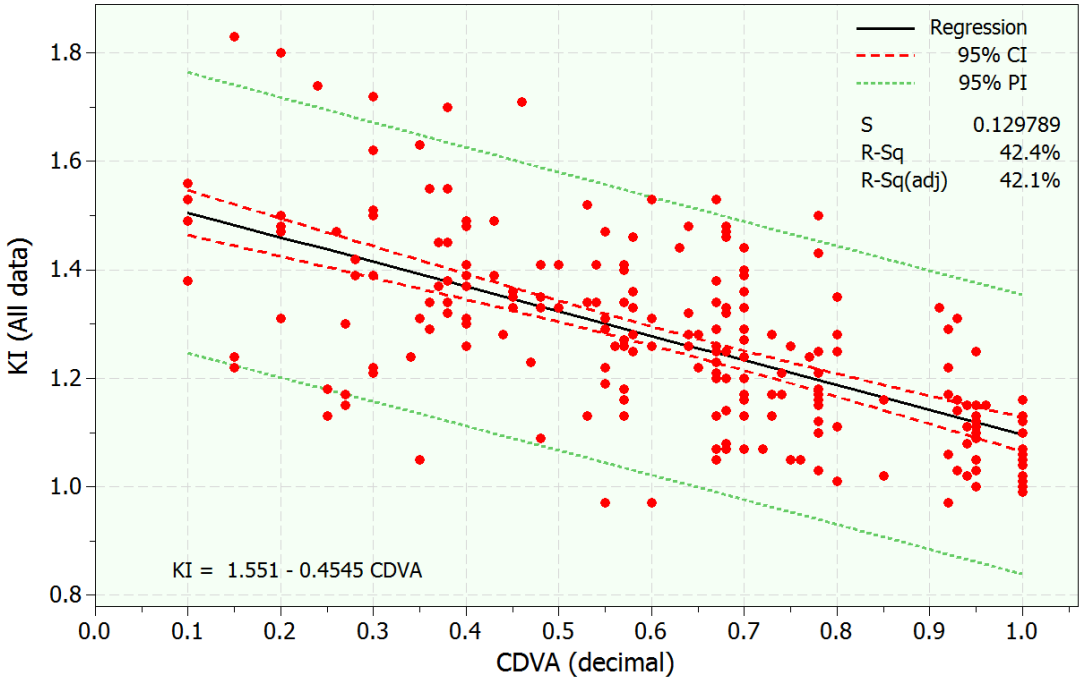

1d CKI (Central Keratoconus Index) vs CDVA

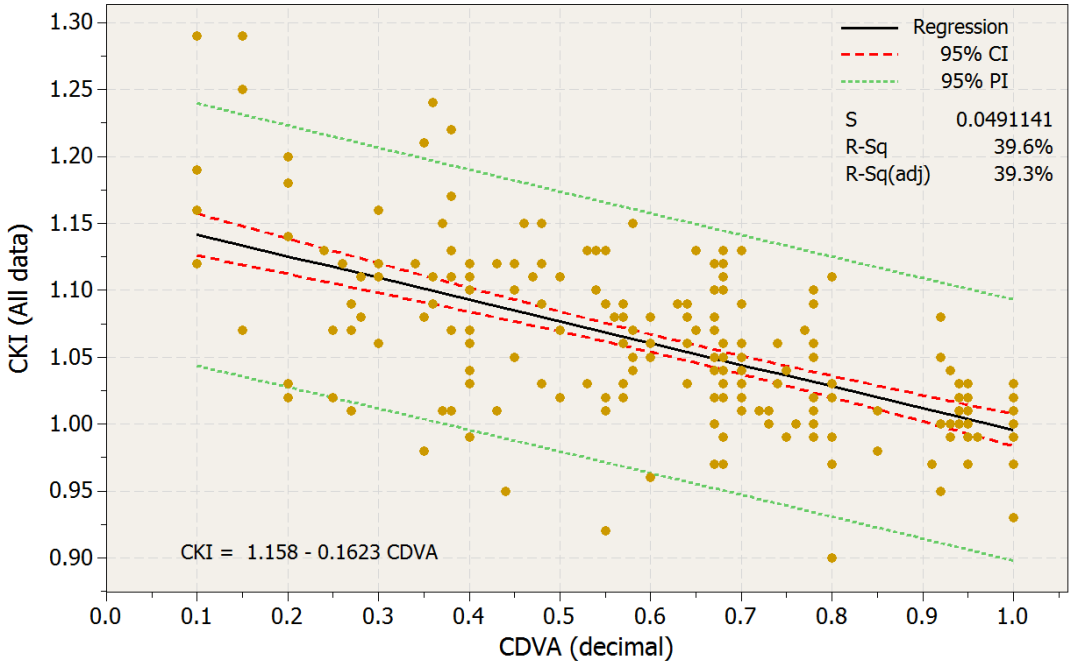

1e IHA (Index of Height Asymmetry) vs CDVA

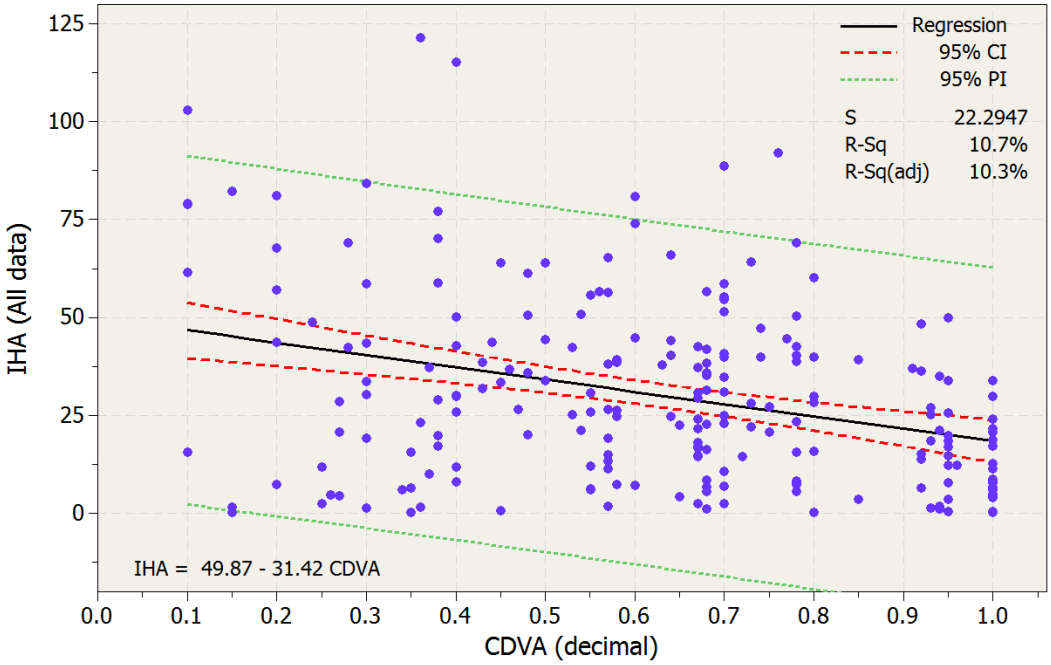

1f IHD (Index of Height Decentration) vs CDVA

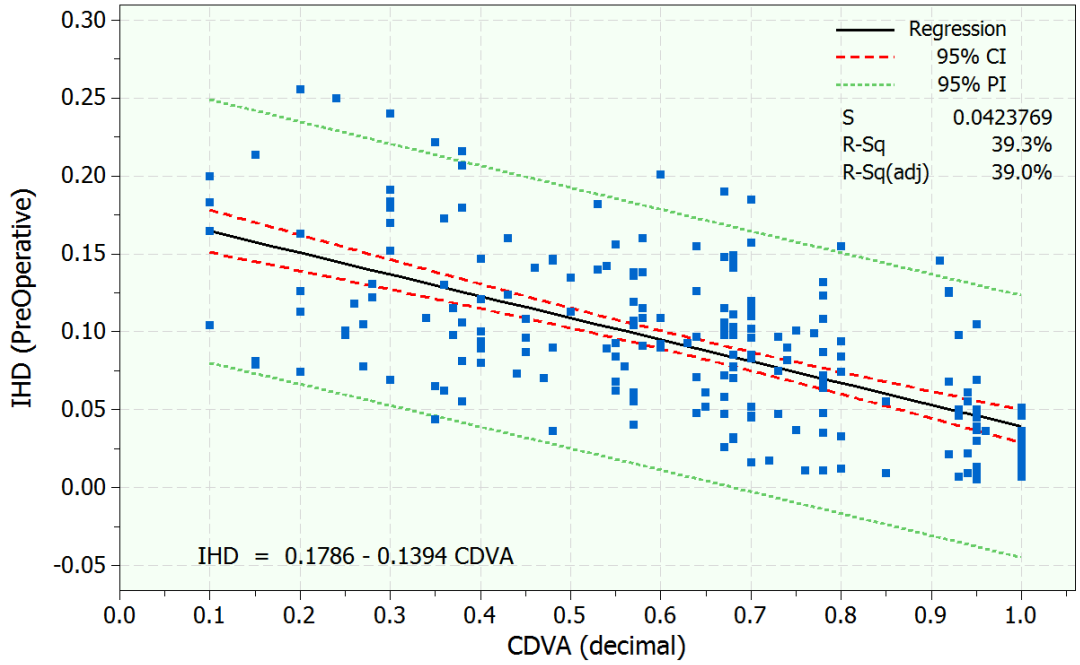

1g R min (minimum radius of curvature) vs CDVA

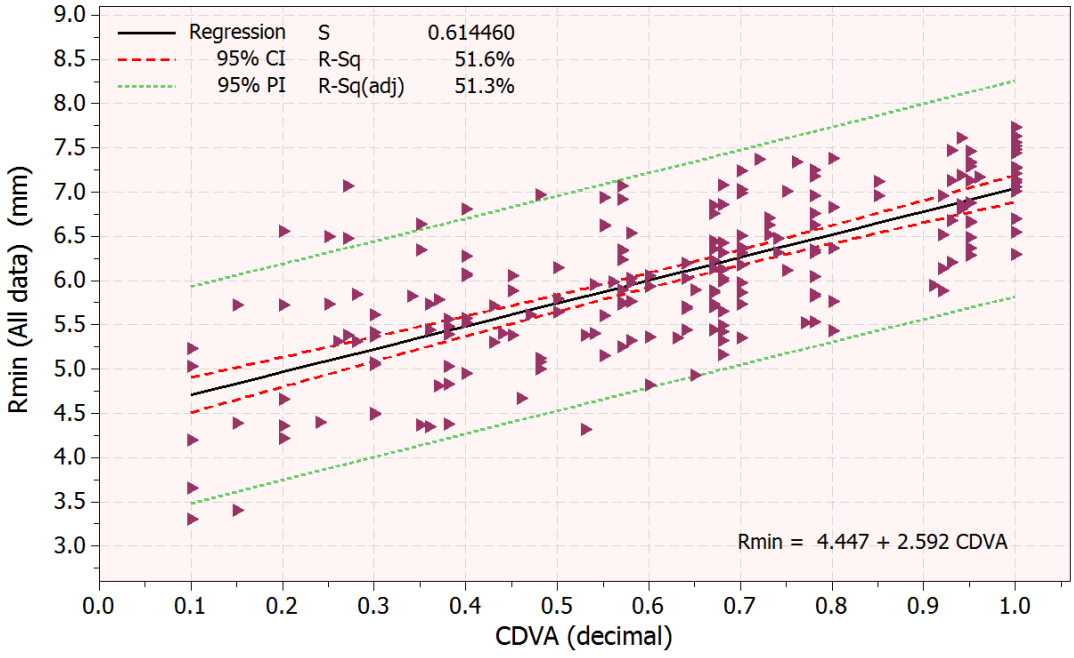

Figure 2

Box plots of measured parameters vs keratoconus grading, as produced by the Oculyzer software showing median level (indicated by ⊗), average symbol (⊕), 95% median confidence range box (black line boxes), and interquartile intervals range box (red line boxes).

2a: best spectacle-corrected distance visual acuity (CDVA) vs keratoconus grading

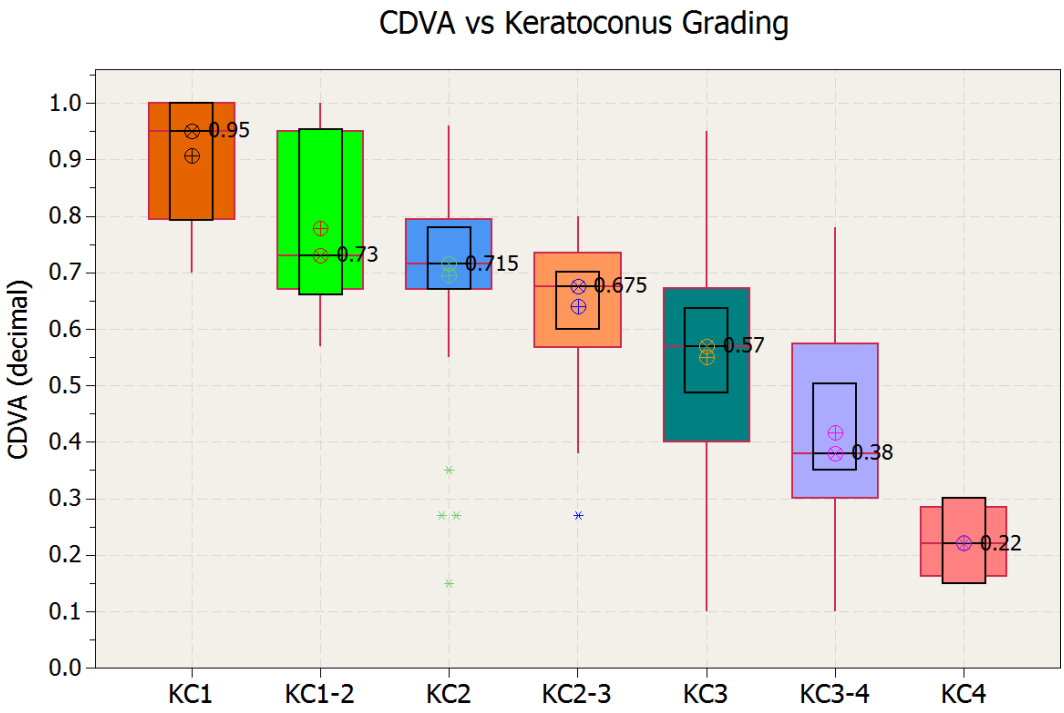

2b: ISV (Index of Surface Variance) vs keratoconus grading

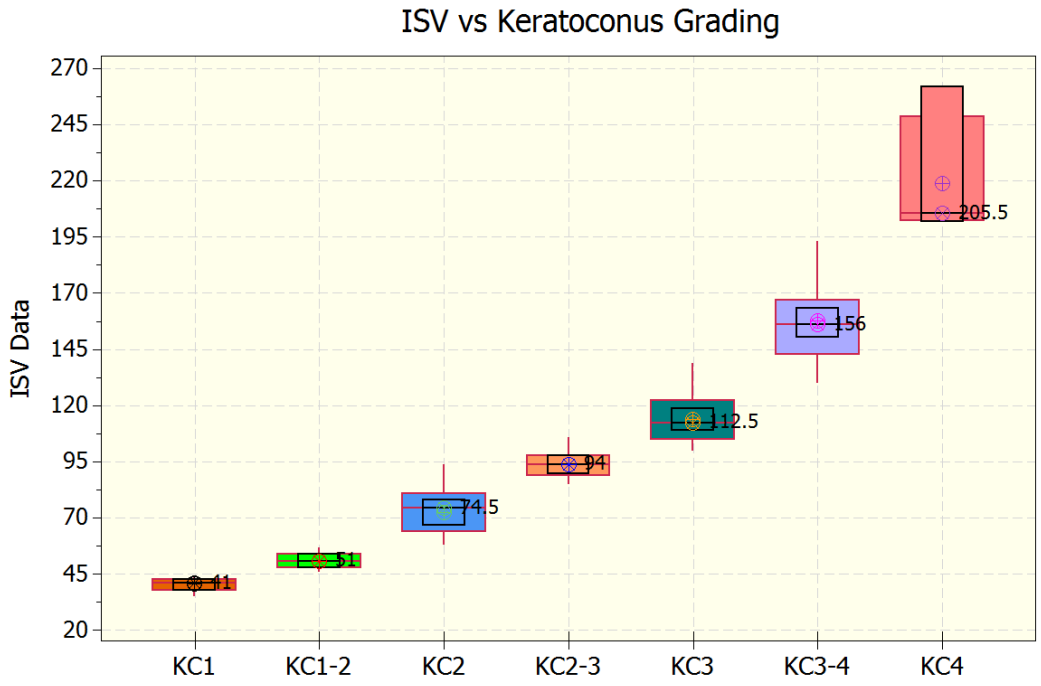

2c: IVA (Index of Vertical Asymmetry) vs keratoconus grading

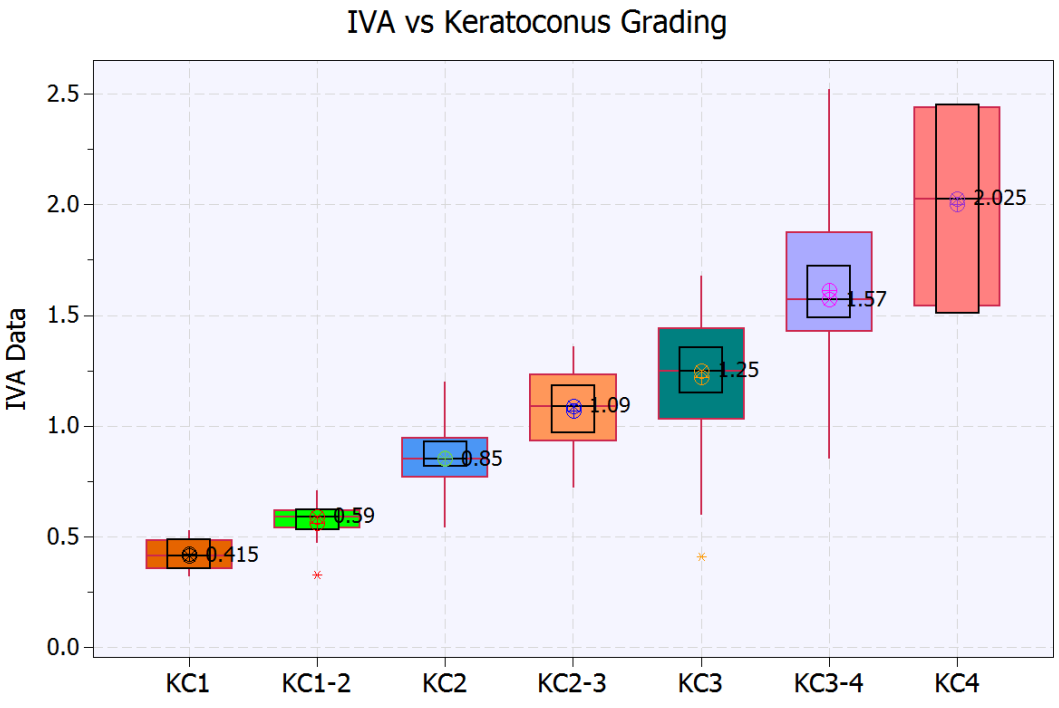

2d: KI (Keratoconus Index) vs keratoconus grading

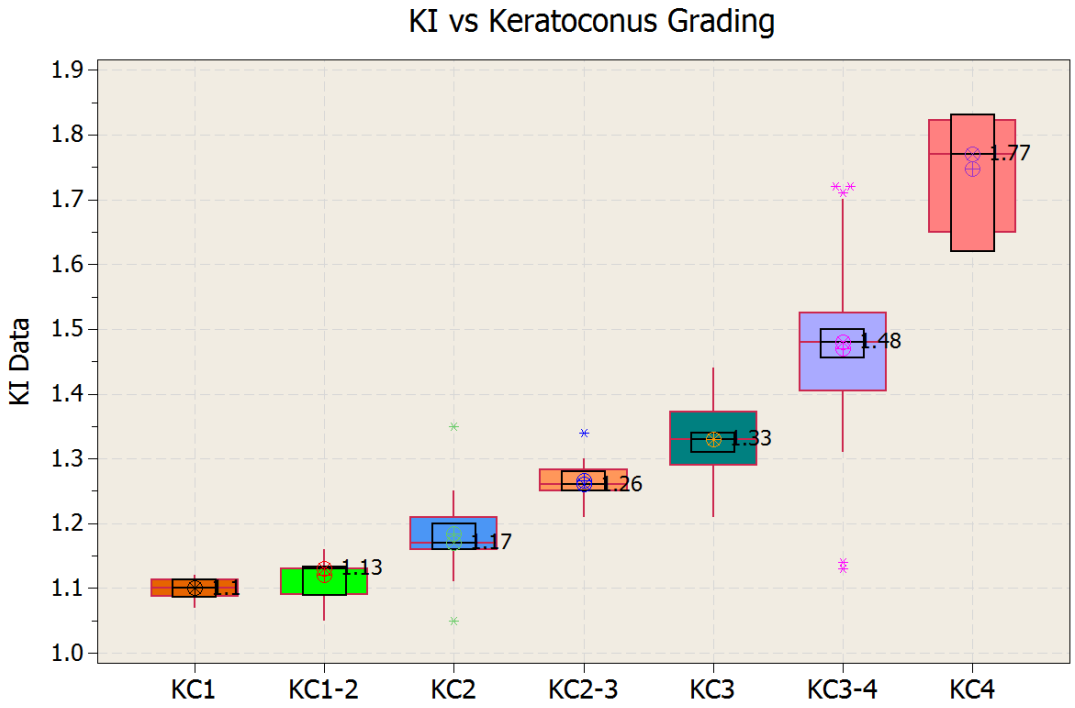

2e: CKI (Central Keratoconus Index) vs keratoconus grading.

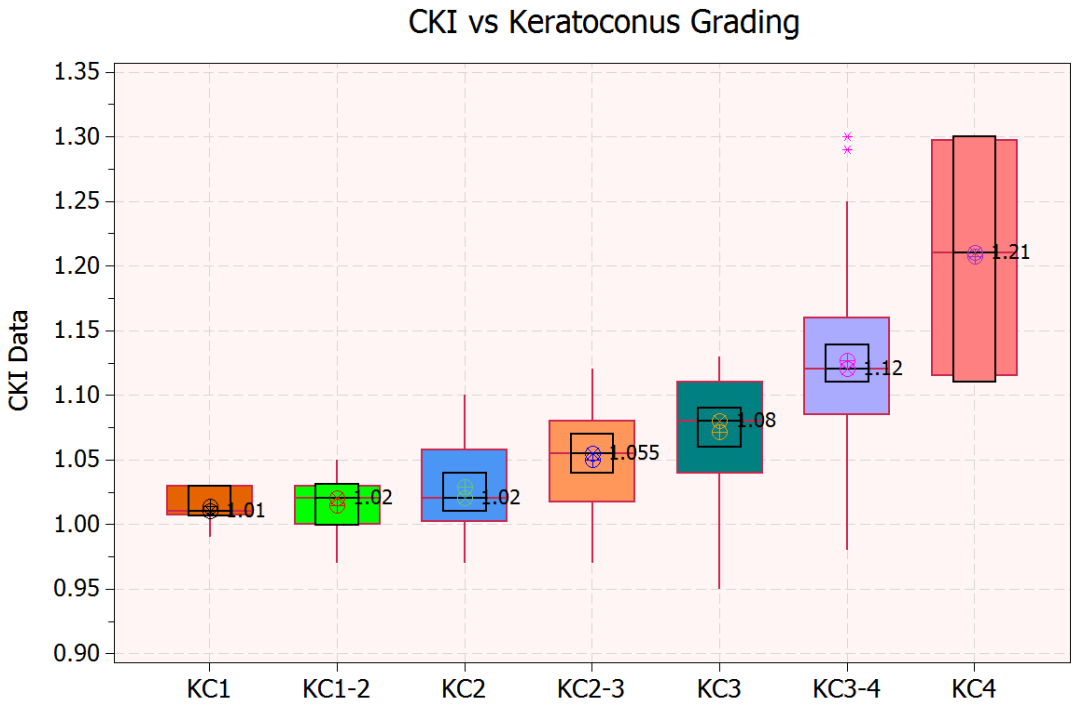

2f: IHA (Index of Height Asymmetry) vs keratoconus grading.

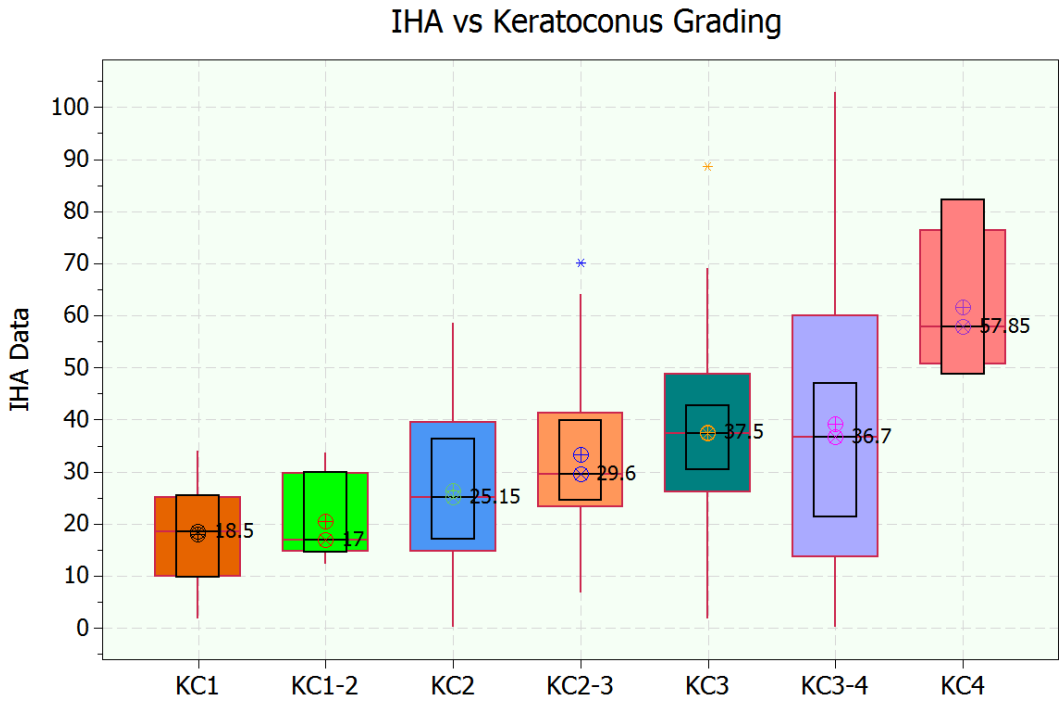

2g: IHD (Index of Height Decentration) vs keratoconus grading,

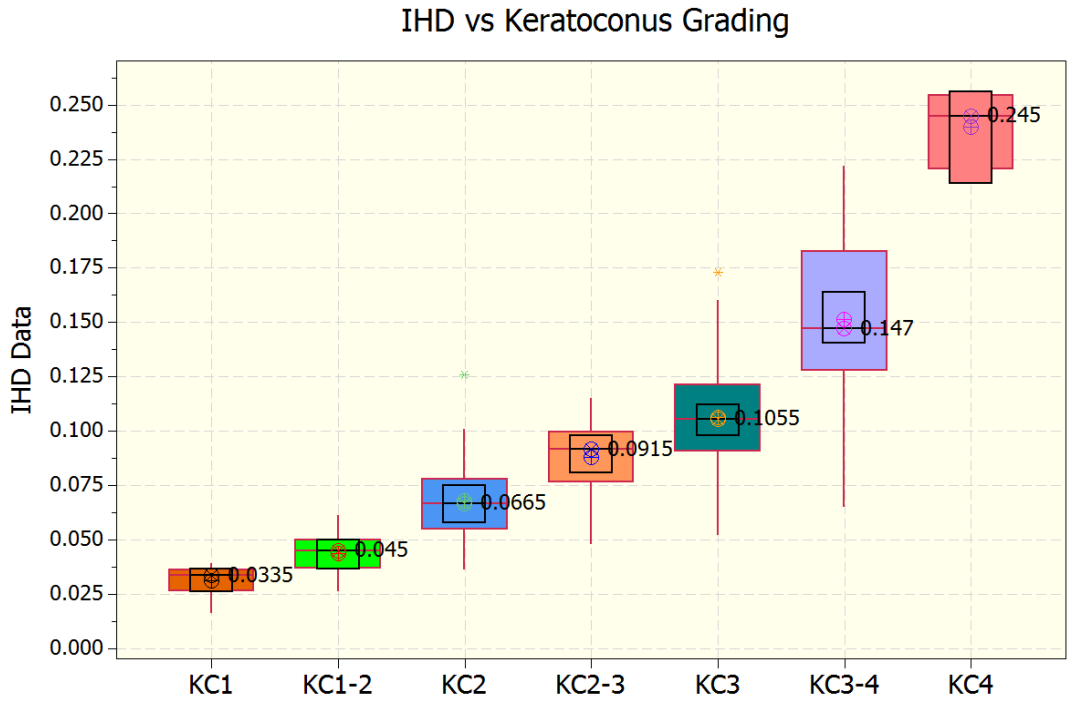

2h: R min (minimum radius of curvature) vs keratoconus grading,

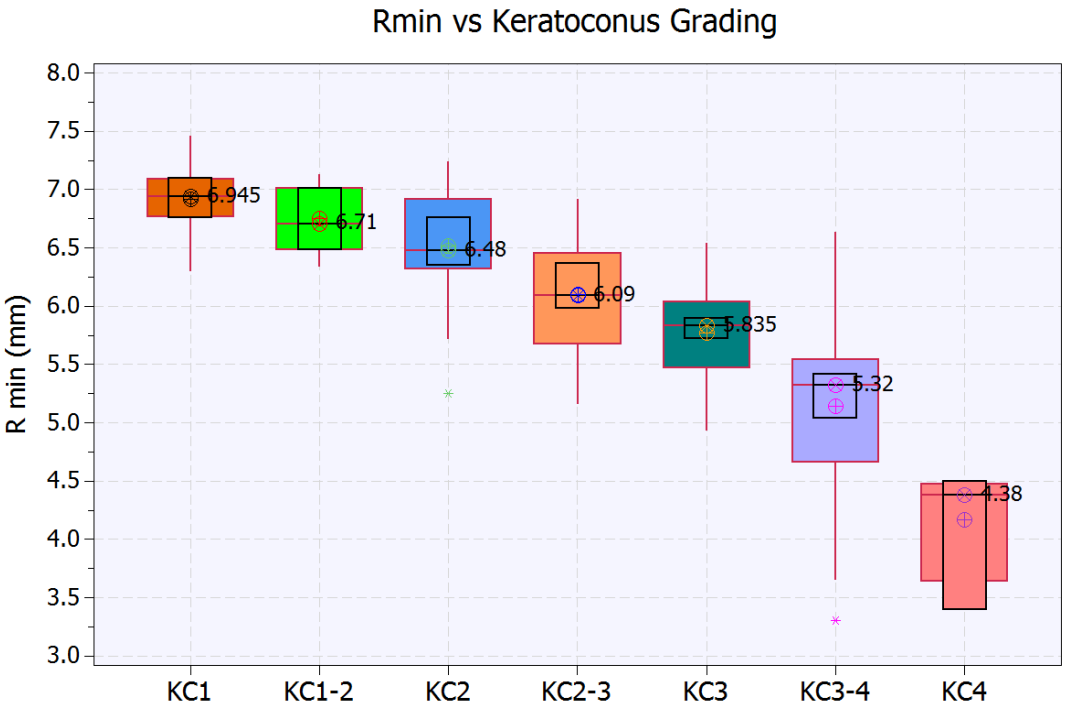

References

1. Krachmer JH, Feder RS, Belin MW. Keratoconus and related noninflammatory corneal thinning disorders. *Surv Ophthalmol*. 1984;28(4):293-322.

2. Belin MW, Asota IM, Ambrosio R Jr, Khachikian SS. What's in a name: keratoconus, pellucid marginal degeneration, and related thinning disorders. *Am J Ophthalmol.* 2011;152(2):157-162

3. Ambrósio R, Caldas DL, da Silva RS, Pimentel LN, de Freitas VB. Impact of the wavefront analysis in refraction of keratoconus patients. 2010 Rev. *Bras. Oftalmol*. 2010; 69 (5): 294-300

4. Kosaki R, Maeda N, Bessho K, Hori Y, Nishida K, Suzaki A, Hirohara Y, Mihashi T, Fujikado T, Tano Y. Magnitude and orientation of Zernike terms in patients with keratoconus. *Invest Ophthalmol Vis Sci.* 2007;48(7):3062-8.

5. Zadnik K, Steger-May K, Fink BA, Joslin CE, Nichols JJ, Rosenstiel CE, Tyler JA, Yu JA, Raasch TW, Schechtman KB; CLEK Study Group. Collaborative Longitudinal Evaluation of Keratoconus. Between-eye asymmetry in keratoconus. *Cornea*. 2002;21(7):671-9.

6. Jones-Jordan LA, Walline JJ, Sinnott LT, Kymes SM, Zadnik K. Asymmetry in keratoconus and vision-related quality of life. *Cornea.* 2013;32(3):267-72.

7. Randleman JB, Trattler WB, Stulting RD. Validation of the ectasia risk score system for preoperative laser in situ keratomileusis screening. *Am J Ophthalmol* 2008;145:813-8.

8. Rabinowitz YS. Videokeratographic indices to aid in screening for keratoconus. *J Refract Surg.* 1995;11:371–9

9. Abad JC, Rubinfeld RS, Del Valle M, Belin MW, Kurstin JM. Vertical D: A novel topographic pattern in some keratoconus suspects. *Ophthalmology* 2007;114:1020-6.

10. Ambrosió R, Simonato R, Luz A, Coca Velarde LG. Corneal-thickness spatial profile and corneal-volume distribution: Tomographic indices to detect keratoconus. *J Cataract Refract Surg.* 2006;32:1851–9

11. McAlinden C, Khadka J, Pesudovs K. A comprehensive evaluation of the precision (repeatability and reproducibility) of the Oculus Pentacam HR. *Invest Ophthalmol Vis Sci* 2011;52(10):7731-37.

12. Swartz T, Marten L, Wang M. Measuring the cornea: the latest developments in corneal topography. *Curr Opin Ophthalmol.* 2007;18(9):325-333.

13. Li X, Yang H, Rabinowitz YS. Keratoconus: classification scheme based on videokeratography and clinical signs. *J Cataract Refract Surg* 2009; 35:1597–1603

14. Greenstein SA, Fry KL, Hersh PS. Corneal topography indices after corneal collagen crosslinking for keratoconus and corneal ectasia: one-year results. *J Cataract Refract Surg.* 2011;37(7):1282-90

15. Sonmez B, Doan MP, Hamilton DR. Identification of scanning slit-beam topographic parameters important in distinguishing normal from keratoconic corneal morphologic features. *Am J Ophthalmol.* 2007;143(3):401-8.

16. Ho JD, Tsai CY, Tsai RJ, Kuo LL, Tsai IL, Liou SW. Validity of the keratometric index: evaluation by the Pentacam rotating Scheimpflug camera. *J Cataract Refract Surg*. 2008;34(1):137-145.

17. Faria-Correia F, Ramos IC, Lopes BT, Salomão MQ, Luz A, Correa RO, Belin MW, and Ambrósio R Jr. Topometric and tomographic indices for the diagnosis of keratoconus. *Int J of Kerat and Ectatic Dis* 2012;1(2):100-06.

18. Rüfer F, Schröder A, Arvani MK, Erb C. Central and peripheral corneal pachymetry-standard evaluation with the Pentacam system [German]. *Klin Monbl Augenheilkd*. 2005;222(2):117-122.

19. Emre S, Doganay S, Yologlu S. Evaluation of anterior segment parameters in keratoconic eyes measured with the Pentacam system. *J Cataract Refract Surg.* 2007;33(10):1708-1712.

20. Zadnik K, Barr JT, Edrington TB, Everett DF, Jameson M, McMahon TT, Shin JA, Sterling JL, Wagner H, Gordon MO. Baseline findings in the collaborative longitudinal evaluation of keratoconus (CLEK) Study. *Invest Ophthalmol Vis Sci* 1998;39(13):2537-46.

21. Kanellopoulos AJ, Asimellis G. Introduction of quantitative and qualitative cornea optical coherence tomography findings induced by collagen cross-linking for keratoconus: a novel effect measurement benchmark. *Clin Ophthalmol* 2013;7:329–335.

22. Gordon-Shaag A, Millodot M, Shneor E. The Epidemiology and Etiology of Keratoconus. *Int J Keratoco Ectatic Corneal Dis.* 2012;1(1):7-15.

23. Krumeich JH, Daniel J, Knulle A. Live-epikeratophakia for keratoconus. *J Cataract Refract Surg* 1998;24:456-63.

24. WaveLight ALLEGRO Oculyzer 1074 User Manual en / Rev.4 / 10-03-02 Item No.: 6654 2001

25. Jafri B, Li X, Yang H, Rabinowitz YS. Higher order wavefront aberrations and topography in early and suspected keratoconus. *J Refract Surg* 2007; 23:774–781

26. Dubbelman M, Weeber HA, van der Heijde RG, Völker-Dieben HJ. Radius and asphericity of the posterior corneal surface determined by corrected Scheimpflug photography. *Acta Ophthalmol Scand.* 2002;80(4):379-83.

27. Maeda N, Klyce SD, Smolek MK, Thompson HW. Automated Keratoconus Screening With Corneal Topography Analysis. *Invest Ophthalmol Vis Sci.* 1994;35(6):2749-57.

28. Ho JD, Tsai CY, Tsai RJ, Kuo LL, Tsai IL, Liou SW. Validity of the keratometric index: evaluation by the Pentacam rotating Scheimpflug camera. *J Cataract Refract Surg.* 2008;34(1):137-45.

29. Bernardo T, Lopes BT, Ramos IC, Faria-Correia F, Luz A, Valbon B, Belin MW, and Ambrósio R Jr. Correlation of Topometric and Tomographic Indices with Visual Acuity in Patients with Keratoconus. *Int J of Kerat and Ectatic Dis* 2012;1(3):167-172.

30. Ishii R, Kamiya K, Igarashi A, Shimizu K, Utsumi Y, Kumanomido T. Correlation of corneal elevation with severity of keratoconus by means of anterior and posterior topographic analysis. *Cornea*. 2012;31(3):253-8.

31. Kanellopoulos AJ. Comparison of sequential vs same-day simultaneous collagen cross-linking and topography-guided PRK for treatment of keratoconus. *J Refract Surg.* 2009;25(9):S812-8.

32. Schoneveld P, Pesudovs K, Coster DJ. Predicting visual performance from optical quality metrics in keratoconus. *Clin Exp Optom.* 2009;92(3):289-96.

Topography-guided Hyperopic LASIK With and Without High Irradiance Collagen Cross-linking: Initial Comparative Clinical Findings in a Contralateral Eye Study of 34 Consecutive Patients

Anastasios John Kanellopoulos, MD; Jonathan Kahn, MD

ABSTRACT

PURPOSE: To evaluate the safety and efficacy of intrastromally applied collagen cross-linking (CXL) in a comparative contralateral eye study of topography-guided femtosecond laser–assisted hyperopic LASIK.

METHODS: Thirty-four consecutive patients with hyperopia and hyperopic astigmatism elected to have bilateral topography-guided LASIK and were randomized to receive a single drop of 0.1% sodium phosphate riboflavin solution under the flap followed by 3-minute exposure of 10 mW/cm^2 ultraviolet A (UVA) light with the flap realigned in one eye (CXL group) and no intrastromal CXL in the contralateral eye (no CXL group). All eyes were treated with the WaveLight FS200 femtosecond laser and WaveLight EX500 excimer laser (Alcon Laboratories Inc). Refractive error and keratometric, topographic, and tomographic measurements were evaluated over mean follow-up of 23 months.

RESULTS: Preoperatively, mean spherical equivalent refraction was +3.15±1.46 diopters (D) and +3.40±1.78 D with a mean cylinder of 1.20±1.18 D and 1.40±1.80 D and mean uncorrected distance visual acuity (UDVA) (decimal) of 0.1±0.26 and 0.1±0.25 in the CXL and no CXL groups, respectively. At 2 years postoperatively, mean spherical equivalent refraction was −0.20±0.56 D and +0.20±0.40 D with mean cylinder of 0.65±0.56 D and 0.76±0.72 D and mean UDVA of 0.95±0.15 and 0.85±0.23 in the CXL and no CXL groups, respectively. Eyes with CXL demonstrated a mean regression from treatment of +0.22±0.31 D, whereas eyes without CXL showed a statistically significant greater regression of +0.72±0.19 D (*P*=.0001).

CONCLUSIONS: Topography-guided hyperopic LASIK with or without intrastromal CXL is safe and effective, with greater long-term efficacy (less regression) in eyes with CXL. Our data suggest that the regression seen with hyperopic LASIK may be related to biomechanical changes in corneal shape over time. [*J Refract Surg*. 2012;28(11 Suppl):S837-S840.]

doi:10.3928/1081597X-20121005-05

The evolution of laser vision correction technology has made the treatment of myopia, hyperopia, and astigmatism more accurate. Numerous studies of hyperopic LASIK have been reported,[1-7] and as the WaveLight Allegretto Wave laser (Alcon Laboratories Inc, Ft Worth, Texas) was introduced, reports of wavefront-optimized hyperopic LASIK have also been published.[8,9] We previously reported the use of topography-guided excimer laser ablations for hyperopia and their advantage in correcting angle kappa.[10,11]

Recently, we published a report on a large cohort of topography-guided hyperopic LASIK with long-term follow-up.[12] In this study, we found a higher level of safety and efficacy when treating hyperopia and hyperopic astigmatism with topography-guided LASIK. Nevertheless, between 1 and 2 years postoperatively a consistent level of regression was noted. We theorized that this was due to a progressive flattening effect, and not due to latent hyperopia and/or accommodation loss, because the regression was consistent with a reduction of the amount of "steepening" of corneal shape achieved initially.

We also introduced the concept of high irradiance, short exposure corneal collagen cross-linking (CXL)[13] and prophylactic CXL in myopic LASIK several years ago,[14] and recently reported the long-term safety and efficacy of these therapies. In the present study, we have attempted to evaluate the effect of "prophylactic" CXL in the long-term stability and safety of hyperopic topography-guided LASIK.

PATIENTS AND METHODS

All patients signed informed consent prior to treatment following the protocol set forth by the Declaration of Helsinki.

From the Department of Ophthalmology, New York University Medical School, New York, New York (Kanellopoulos, Kahn); and LaserVision.gr Eye Institute, Athens, Greece (Kanellopoulos).

Dr Kanellopoulos is a consultant to Alcon Laboratories Inc. Dr Kahn has no financial interest in the materials presented herein.

Presented in part at the American Society of Cataract and Refractive Surgery annual meeting; April 20-24, 2012; Chicago, Illinois.

Correspondence: Anastasios John Kanellopoulos, MD, LaserVision.gr Eye Institute, Tsocha 17 Ampelokipi, 11527, Athens, Greece. Tel: 30 210 7472 777; Fax: 30 210 7472 789; E-mail: ajk@brilliantvision.com

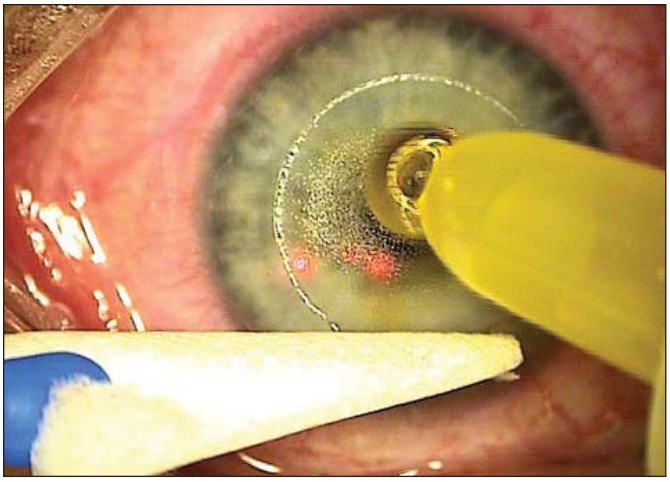

Figure 1. Riboflavin is instilled on the bare stromal bed. Care is taken to avoid contact with the folded LASIK flap.

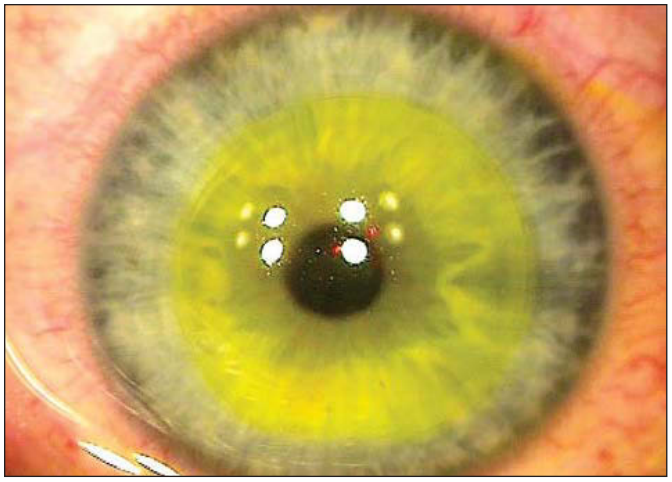

Figure 2. Repositioned LASIK flap. The yellow tinge seen within the corneal stroma is the riboflavin.

Thirty-four patients (68 eyes) underwent bilateral topographic-guided hyperopic LASIK in our facility from March 2010 to October 2010, with one eye randomized (by coin toss) to receive prophylactic instrastromal CXL. Inclusion criteria were hyperopia of +0.25 to +8.00 diopters (D) and astigmatism up to −6.00 D with a spherical equivalent cycloplegic refraction ≤6.00 D. Exclusion criteria were previous corneal surgery, history of herpetic eye disease, corneal dystrophy, corneal scarring, keratoconus, severe dry eye, or collagen vascular diseases.

Preoperative evaluation included uncorrected distance visual acuity (UDVA), refraction (cycloplegic), corrected distance visual acuity (CDVA), slit-lamp examination including fundus evaluation, corneal imaging with Scheimflug corneal tomography (Oculyzer II, Alcon Laboratories Inc) and Placido disc–based topography (Vario, Alcon Laboratories Inc), ultrasound central corneal pachymetry with the NIDEK US-1800 (Echoscan, Achi, Japan), and wavefront analysis with the Allegretto-Wave Tscherning wavefront analyzer (WaveLight Technologie AG, Erlangen, Germany) measured at 6.5-mm pupil size. Contrast sensitivities were also measured using CSV-1000 (VectorVision, Arcanum, Ohio).

A custom nomogram-adjustment algorithm for determining the ablation treatment plan was used per our previous experience. As an important differentiator, this algorithm was used to compensate for the regression encountered in earlier cases; however, this nomogram-adjusted algorithm was not used in eyes randomized to receive intrastromal CXL.

Surgical Technique

A disposable patient interface was used for flap creation in each eye treated with the FS200 femtosecond laser (Alcon Laboratories Inc). One drop of proparacaine 1% (Alcaine, Alcon Laboratories Inc) was instilled in the patient's eye just before the procedure. Eyelids were painted with povidone iodine antiseptic 10% (Betadine; Purdue Pharma L.P., Stamford, Connecticut), and the eye lashes were isolated with sterile plastic drapes (Tegaderm; 3M Health Care, St Paul, Minnesota). The femtosecond laser was used to cut the corneal flaps in all cases. The flaps were cut to expose a stromal bed at a diameter of at least 9.0 mm and depth of 135 µm, which was sufficiently large for the hyperopic (large diameter) ablation and its accompanying blend zone. The intraoperative flap diameter was measured with a surgical caliper, and pachymetry measurement of the residual stromal bed was done with the built-in optical pachymeter of the EX500. The 500-Hz EX excimer laser was used to perform the ablations in all cases using the topography-guided platform. Images were taken from the Oculyzer II as described previously.[12]

At the completion of the excimer ablation, eyes that were randomized to receive CXL were given one drop of our custom 0.1% riboflavin sodium phosphate solution (Leiter's Pharmacy, San Francisco, California), on the bare stromal bed, which was left to soak for 60 seconds. Special care was taken not to allow the riboflavin solution to come in contact with the already folded LASIK flap (Fig 1). After 60 seconds of soaking, the LASIK flap was reflected into place and copiously irrigated and "ironed" in place with a Johnston applanator (Rhein Medical, Tampa, Florida) (Fig 2).

Immediately afterwards, one drop of Vigamox solution (Alcon Laboratories) was applied to the cornea and it was illuminated with 10 mW/cm^2 of 370-nm UV light with the KXL device (Avedro, Waltham, Massachusetts) for a total of 3 minutes. No additional drops

Copyright © SLACK Incorporated

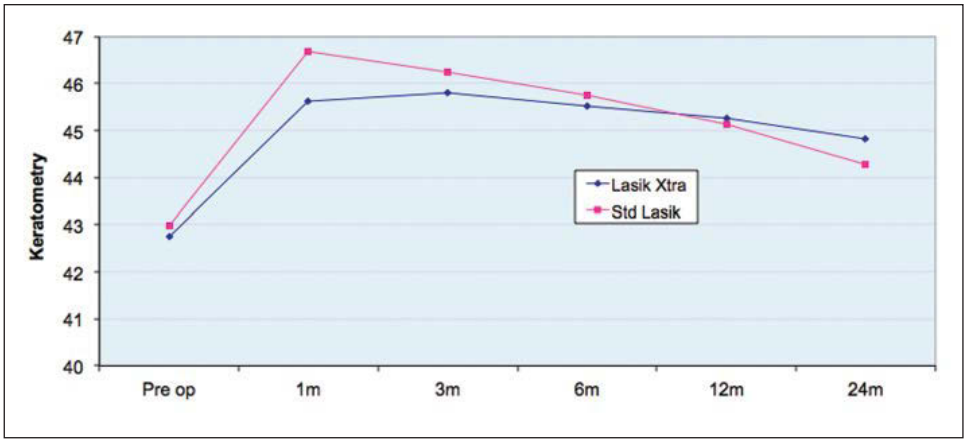

Figure 3. Pre- and postoperative comparison of the mean keratometric change in hyperopic eyes with intrastromal cross-linking (LASIK Xtra) and those without (Std LASIK) (*P*=.001).

of riboflavin were administered. The surface was kept moist with two to three drops of Vigamox during the 3-minute interval. A bandage contact lens was placed on the ocular surface, and the patient was prescribed Vigamox and 1% prednisolone acetate (PredForte; Allergan, Irvine, California) four times a day for 1 week. Patients were examined 30 minutes postoperatively to check for any flap irregularities or complications.

Postoperatively, UDVA, CDVA, corneal tomography and topography, and manifest and cycloplegic refraction were evaluated. These examinations were repeated during follow-up at 1 day, 1 week, and 1, 3, and 6 months, and every 6 months thereafter. All surgeries were performed by a single surgeon (A.J.K.) in an outpatient refractive surgery center in Athens, Greece. Measurements and data were obtained by the surgeon and his associate staff.

RESULTS

Preoperatively, mean spherical equivalent cycloplegic refraction (SE) was +3.15±1.46 D and +3.40±1.78 D with mean cylinder of 1.20±1.18 D and 1.40±1.80 and mean decimal UDVA of 0.1±0.26 and 0.1±0.25 in the CXL and no CXL groups, respectively. Postoperatively, mean SE at 2-year follow-up was −0.20±0.56 D and +0.20±0.40 D with mean cylinder of 0.65±0.56 D and 0.76±0.72 D and mean decimal UDVA of 0.95±0.15 and 0.85±0.23 in the CXL and no CXL groups, respectively. Eyes with intrastromal CXL demonstrated a mean regression from treatment of +0.22±0.31, whereas the eyes that did not receive CXL showed a statistically significant greater regression of +0.72±0.19 (*P*=.0001).

Figure 3 shows the pre- and postoperative comparison of the mean keratometric change for each group. Overcorrection was seen in the no CXL group, as expected due to the added +0.50 D in the nomogram adjustment for this group, which seemed to decrease over the 2-year follow-up period. In eyes that received adjunct intrastromal CXL, no overcorrection was noted and greater stability was achieved.

DISCUSSION

In previous studies, the potential advantage of using a topography-guided ablation profile in the correction of hyperopic refractive errors has been demonstrated with greater importance than myopic errors because of the presence of angle kappa in hyperopes.[11] When treating with wavefront-optimized or wavefront-guided ablation, the treatment pattern is centered on the entrance pupil, whereas with topographic-guided ablation, it is centered on the corneal apex. Although much debate surrounds the best location for centration, evidence suggests that the corneal apex may be more closely aligned to the visual axis, especially when compensating for angle kappa in hyperopes.[15]

In this study, we sought to evaluate the stability of these results after using intrastromal CXL. This, in theory, would act as a biomechanical modulator to the intrinsic corneal flattening response of hyperopic LASIK seen during long-term follow-up. The keratometric regression noted over the 2 years of follow-up in the eyes randomized to not receive adjunctive intrastromal CXL confirms, in our opinion, the above-mentioned intrinsic biomechanical mechanism of regression in hyperopic LASIK. We believe this to be an "expansion" or "stretching" of the severed midperipheral corneal fibers that have been ablated, resulting in progressive flattening of the steepened central cornea. Although the possibility of midperipheral thickening and central thinning of the epithelium might also play a role in the regression, the fact that it was statistically minimized in the eyes undergoing intrastromal CXL points more clearly to the biomechanical mechanism.

The implication of biomechanical modulation of postoperative hyperopic LASIK regression, so as to prevent progressive refractive instability over time, sets a new level of dynamic control on the outcomes of

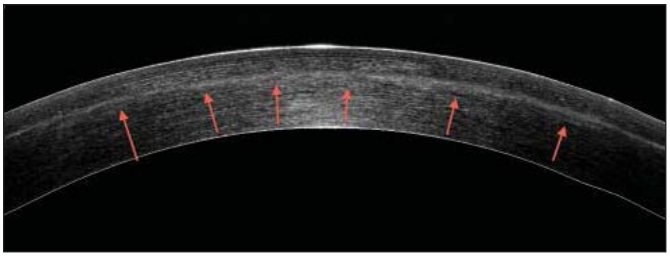

Figure 4. Corneal optical coherence tomography scan taken 3 months postoperatively of an eye that received intrastromal cross-linking (CXL) during hyperopic LASIK. The hyperreflective area around the LASIK flap interface (arrows) demonstrates the achieved CXL effect.

laser vision correction surgery, which previously was restricted to a static change in refractive error. Just as the dynamic change of refraction seen with progressive keratoconus requires CXL to prevent the instability and irregularity of ectasia, in a similar way, the dynamic refractive and topographic regression of hyperopic LASIK now seems to require CXL to maintain stability over time. This also may be true of myopic regression seen in high myopic treatments with thin corneas, and is the reason why some have advocated LASIK Xtra (LASIK + intrastromal CXL) for higher risk eyes.[14,16]

Our preliminary data suggest that the combination of high irradiance, short exposure intrastromal CXL may offer a significant synergy in maintaining the long-term efficacy and stability of topography-guided hyperopic LASIK (Fig 4). However, we are unable to know or predict with certainty what will occur past 2 years based on these data. This synergy suggests that the regression of effect in hyperopic LASIK may be more related to corneal biomechanical changes than just a loss of residual accommodation, lens changes, or epithelial thickening. The use of CXL in association with LASIK may become another significant application of corneal CXL and further expand the science of modulating biomechanical change in refractive surgery.[17] Finally, topography-guided LASIK with the EX500 excimer laser and FS200 femtosecond laser, with and without adjunctive intrastromal CXL, appears to be safe and effective in the correction of hyperopia and hyperopic astigmatism.

AUTHOR CONTRIBUTIONS

Study concept and design (A.J.K.); data collection (A.J.K.); analysis and interpretation of data (A.J.K., J.K.); drafting of the manuscript (A.J.K.); critical revision of the manuscript (A.J.K., J.K.); statistical expertise (A.J.K.); administrative, technical, or material support (A.J.K.); supervision (A.J.K.)

REFERENCES

1. Salz JJ, Stevens CA; LADARVision LASIK Hyperopia Study Group. LASIK correction of spherical hyperopia, hyperopic astigmatism, and mixed astigmatism with the LADARVision excimer laser system. *Ophthalmology*. 2002;109(9):1647-1656.
2. Lian J, Ye W, Zhou D, Wang K. Laser in situ keratomileusis for correction of hyperopia and hyperopic astigmatism with the Technolas 117C. *J Refract Surg*. 2002;18(4):435-438.
3. Carones F, Vigo L, Scandola E. Laser in situ keratomileusis for hyperopia and hyperopic and mixed astigmatism with LADARVision using 7 to 10-mm ablation diameters. *J Refract Surg*. 2003;19(5):548-554.
4. Pineda-Fernandez A, Rueda L, Huang D, Nur J, Jaramillo J. Laser in situ keratomileusis for hyperopia and hyperopic astigmatism with the Nidek EC-5000 excimer laser. *J Refract Surg*. 2001;17(6):670-675.
5. Goldberg DB. Comparison of myopes and hyperopes after laser in situ keratomileusis monovision. *J Cataract Refract Surg*. 2003;29(9):1695-1701.
6. Ditzen K, Fiedler J, Pieger S. Laser in situ keratomileusis for hyperopia and hyperopic astigmatism using the Meditec MEL 70 spot scanner. *J Refract Surg*. 2002;18(4):430-434.
7. Oshika T, Klyce SD, Applegate RA, Howland HC, El Danasoury MA. Comparison of corneal wavefront aberrations after photorefractive keratectomy and laser in situ keratomileusis. *Am J Ophthalmol*. 1999;127(1):1-7.
8. Kanellopoulos AJ, Conway J, Pe LH. LASIK for hyperopia with the WaveLight excimer laser. *J Refract Surg*. 2006;22(1):43-47.
9. Kezirian GM, Moore CR. Stonecipher KG. Four-year postoperative results of the US ALLEGRETTO WAVE clinical trial for the treatment of hyperopia. *J Refract Surg*. 2008;24(4):S431-S438.
10. Kanellopoulos AJ. Topography-guided custom retreatments in 27 symptomatic eyes. *J Refract Surg*. 2005;21(5):S513-S518.
11. Basmak H, Sahin A, Yildirim N, Papakostas TD, Kanellopoulos AJ. Measurement of angle kappa with synoptophore and Orbscan II in a normal population. *J Refract Surg*. 2007;23(5):456-460.
12. Kanellopoulos AJ. Topography-guided hyperopic and hyperopic astigmatism femtosecond laser-assisted LASIK: long-term experience with the 400 Hz eye-Q excimer platform. *Clin Ophthalmol*. 2012;6:895-901.
13. Kanellopoulos AJ. Long term results of a prospective randomized bilateral eye comparison trial of higher fluence, shorter duration ultraviolet A radiation, and riboflavin collagen cross linking for progressive keratoconus. *Clin Ophthalmol*. 2012;6:97-101.
14. Kanellopoulos AJ. Long-term safety and efficacy follow-up of prophylactic higher fluence collagen cross-linking in high myopic laser-assisted in situ keratomileusis. *Clin Ophthalmol*. 2012;6:1125-1130.
15. Reinstein DZ, Archer TJ, Gobbe M. Is topography-guided ablation profile centered on the corneal vertex better than wavefront-guided ablation profile centered on the entrance pupil? *J Refract Surg*. 2012;28(2):139-143.
16. Celik HU, Alagoz N, Yildirim Y, et al. Accelerated corneal cross-linking concurrent with laser in-situ keratomileusis. *J Cataract Refract Surg*. 2012;38(8):1424-1431.
17. Krueger RR. Biomechanical manipulation: the next frontier in corneal refractive surgery. *J Refract Surg*. 2009;25(10):837-840.

Copyright © SLACK Incorporated